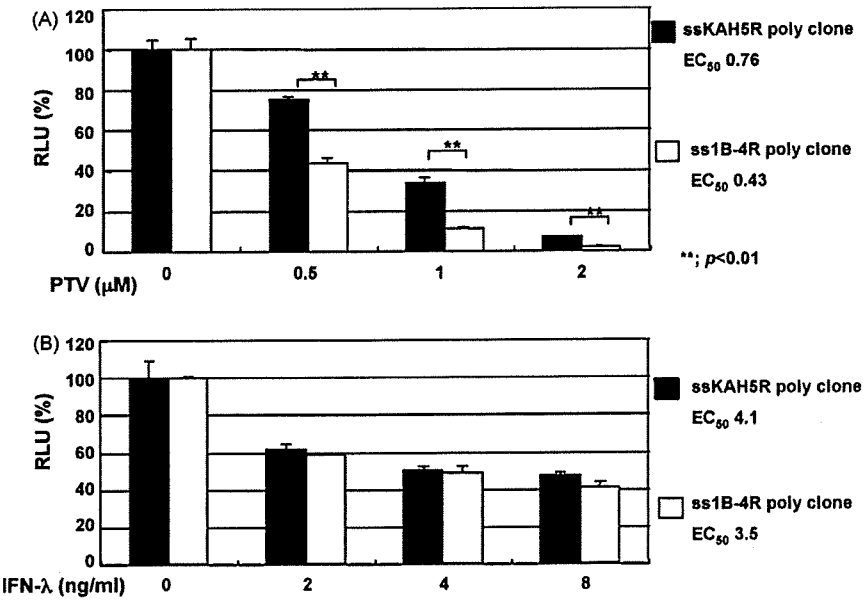


Fig. 9. The sensitivities of the second generation of sKAH5R and s1B-4R to PTV and IFN-λ. Polyclonal second generations of sKAH5R (ssKAH5R) and s1B-4R (ss1B-4R) were treated with PTV (0, 0.5, 1, and 2 μM) (A) and IFN-λ (0, 2, 4, and 8 ng/ml) (B) for 72 h and then were subjected to RL assay. All the luciferase assays were repeated at least three times.

Here, sOR exhibited the lowest level of sensitivity to IFN-α ($EC_{50}$: 2.35 IU/ml). In the clinical setting, high titers of HCV RNA are among the determining factors for IFN resistance. However, the sensitivity to IFN-α was found to be greater in the case of s1B-4R and sKAH5R than in sOR, although HCV RNA titers were higher than those of sOR. These results suggest that factor(s) other than the HCV RNA level may be involved in conferring sensitivity to IFN-α, and the genetic background of sOR may serve as a candidate for interpreting differences in IFN-α sensitivity among the genotype 1b HCVs tested. Previously the structural region of HCV was shown to be involved in viral resistance to type I IFN (Taylor et al., 1999). Therefore, the development of genome-length HCV RNA reporter systems from 1B-4, 1B-5, and KAH5R strains in addition to our developed OR6 cells will overcome the limitation of subgenomic replicon and will become powerful tool for the study of anti-HCV reagents including IFNs. Now we are planning to develop the genome-length HCV RNA reporter systems using these three HCV strains.

sKAH5R exhibited the lowest level of sensitivity to IFN-γ ($EC_{50}$: 2.26 IU/ml) among the replicons tested, as it is approximately 10 times more resistant to IFN-γ than s1B-5R ($EC_{50}$: 0.21 IU/ml). KAH5 was the only HCV strain derived from a patient with AH C in the present study. In our previous study, an AH1 strain derived from a patient with AH C also exhibited lower sensitivity to IFN-γ ($EC_{50}$: 1.9 IU/ml) than did O strain ($EC_{50}$: 0.3 IU/ml) in the genome-length HCV RNA replication system (Mori et al., 2008). In both subgenomic and genome-length HCV RNA replication systems, HCV strains from patients with AH C possess less sensitivity to IFN-γ than do HCV strains from healthy carriers. These results suggest that the NS region of HCV derived from AH C may be involved in IFN-γ resistance.

In 2003, IFN-λ was identified by two groups at the same time, and this novel IFN was classified as type III IFN. IFN-λ shares the Jak/Stat signaling pathway with the type I IFNs, although they bind to distinct membrane receptors, i.e., type I IFNs bind to the heterodimer of IFNAR1 and IFNAR2, whereas type III IFNs bind to the heterodimer of IFNLR1 and IL10R2 (Uze and Monneron, 2007). Therefore, we expected to obtain similar IFN-α sensitivity results in the four replicons tested here. However, unexpectedly, the profiles of replicon sensitivity to IFN-α and IFN-λ differed. The sensitivity of s1B-4R to IFN-λ was approximately five times greater than that of sKAH5R, although the sensitivities of these replicons to IFN-α were almost identical. There are several possible interpretations of these unexpected findings. First, an unidentified branched signaling pathway may account for variation in the anti-HCV activity of IFN-λ. Second, expression levels of the receptor for IFN-λ may vary. The second generation replicon assays suggest that the cellular factors may be dominant in the sensitivity to IFN-λ. Further study will be needed to clarify this issue. The anti-HCV activity of IFN-λ has already been reported by several groups using HCV RNA-harboring cells (Doyle et al., 2006; Marcello et al., 2006; Robek et al., 2005). The present study was the first to demonstrate the diverse anti-HCV activities of IFN-λ on HCV replicons.

In the case of CsA, we did not observe any significant differences among the genotype 1b replicons. Using a genome-length HCV RNA replication system, we recently demonstrated that an AH1 strain obtained from an AH C patient showed greater sensitivity than did an O strain (Mori et al., 2008). There are two possible explanations for this high sensitivity to CsA in the replicon derived from the AH C case: first, a high degree of sensitivity to CsA may not be a common feature in HCV from AH C and may instead be strain-dependent; second, a particular structural region of HCV from AH C may be responsible for this high level of sensitivity to CsA. However, further study will be needed to fully account for these findings.

Respectively, sKAH5R and s1B-4R exhibited the lowest ($EC_{50}$: 1.00 μM) and highest ($EC_{50}$: 0.40 μM) levels of sensitivity to PTV among the replicons tested. We also confirmed that sKAH5R and s1B-4R possessed the lowest and highest levels of sensitivity, respectively in both FLV and RSV treatment. Therefore, resistance to statins may be a unique feature of sKAH5R. It should be noted that we obtained these results using polyclonal sKAH5R and polyclonal s1B-4R cells. The polyclonal sKAH5R cells were less sensitive to PTV, FLV, and RSV than were the polyclonal s1B-4R cells. Therefore, the statin-resistant phenotype of sKAH5R cells is due to a KAH5 strain-specific characteristic, rather than to the clonality of the cells. The second generation of replicon harboring cells, ssKAH5R and ss1B-4R, further supported that the viral factor plays the major role in the statin-resistant phenotype of sKAH5R. These two cell lines with contrasting sensitivity to statins promise to be useful for

determining the statin resistance-responsible region of HCV and also for investigating the anti-HCV mechanism of statins in general.

In the present study, we demonstrated the diverse profiles of four HCV replicons to anti-HCV reagents. sKAH5R showed the lowest sensitivity to IFN-γ, IFN-λ, and statins (PTV, RSV, and FLV). In contrast, s1B-4R exhibited the highest level of sensitivity to IFN-λ and statins (PTV, RSV, and FLV). sKAH5R and s1B-4R possessed a sensitive and a resistant phenotype to various anti-HCV reagents. The nucleotide sequences in the NS3-NS5B regions of 1B-4, 1B-5, and KAH5 strains showed differences of 6.5%, 8.6%, and 6.1%, respectively, from those of the O strain. Similarly, the amino acid sequences in the NS3–NS5B regions of 1B-4, 1B-5, and KAH5 strains showed differences of 2.6%, 4.7%, and 2.5%, respectively, from those of the O strain. Phylogenetic analysis revealed that O, 1B-4, and KAH5 strains formed the cluster different from 1B-5 strain (Supplemental Fig. 3). These data indicate that sKAH5R and s1B-4R are at a similar genetic distance from the O strain. These two replicons were also found to possess similar features in terms of HCV RNA expression levels and sensitivity to IFN-α. Therefore, sKAH5R and s1B-4R are expected to be useful tools for comparative analyses of anti-HCV determining factors of HCV, especially as regards IFN-λ and statins.

In conclusion, we established an HCV replicon reporter assay system with four different genotype 1b HCV strains. This replicon system is a useful tool for investigating differences in sensitivity to anti-HCV reagents among genotype 1b HCV strains, and it is expected to increase the rate of resolution of HCV cases otherwise resistant to current IFN therapy.

## Acknowledgements

The authors would like to thank Atsumi Morishita and Takashi Nakamura for their technical assistance. This work was supported by grants-in-aid for a third-term comprehensive 10-year strategy for cancer control and for research on hepatitis from the Ministry of Health, Labor, and Welfare of Japan.

## Appendix A. Supplementary data

Supplementary data associated with this article can be found, in the online version, at doi:10.1016/j.antiviral.2009.01.007.

## References

Blight, K.J., McKeating, J.A., Marcotrigiano, J., Rice, C.M., 2003. Efficient replication of hepatitis C virus genotype 1a RNAs in cell culture. J. Virol. 77, 3181–3190.

Doyle, S.E., Schreckhise, H., Khuu-Duong, K., Henderson, K., Rosler, R., Storey, H., Yao, L., Liu, H., Barahmand-pour, F., Sivakumar, P., Chan, C., Birks, C., Foster, D., Clegg, C.H., Wietzke-Braun, P., Mihm, S., Klucher, K.M., 2006. Interleukin-29 uses a type 1 interferon-like program to promote antiviral responses in human hepatocytes. Hepatology 44, 896–906.

Firpi, R.J., Nelson, D.R., 2007. Current and future hepatitis C therapies. Arch. Med. Res. 38, 678–690.

Ikeda, M., Abe, K., Dansako, H., Nakamura, T., Naka, K., Kato, N., 2005. Efficient replication of a full-length hepatitis C virus genome, strain O, in cell culture, and development of a luciferase reporter system. Biochem. Biophys. Res. Commun. 329, 1350–1359.

Ikeda, M., Abe, K., Yamada, M., Dansako, H., Naka, K., Kato, N., 2006. Different anti-HCV profiles of statins and their potential for combination therapy with interferon. Hepatology 44, 117–125.

Ikeda, M., Kato, N., 2007. Life style-related diseases of the digestive system: cell culture system for the screening of anti-hepatitis C virus (HCV) reagents: suppression of HCV replication by statins and synergistic action with interferon. J. Pharmacol. Sci. 105, 145–150.

Ikeda, M., Kato, N., Mizutani, T., Sugiyama, K., Tanaka, K., Shimotohno, K., 1997. Analysis of the cell tropism of HCV by using in vitro HCV-infected human lymphocytes and hepatocytes. J. Hepatol. 27, 445–454.

Ikeda, M., Yi, M., Li, K., Lemon, S.M., 2002. Selectable subgenomic and genome-length dicistronic RNAs derived from an infectious molecular clone of the HCV-N strain of hepatitis C virus replicate efficiently in cultured Huh7 cells. J. Virol. 76, 2997–3006.

Inoue, K., Umehara, T., Ruegg, U.T., Yasui, F., Watanabe, T., Yasuda, H., Dumont, J.M., Scalfaro, P., Yoshiba, M., Kohara, M., 2007. Evaluation of a cyclophilin inhibitor in hepatitis C virus-infected chimeric mice in vivo. Hepatology 45, 921–928.

Kapadia, S.B., Chisari, F.V., 2005. Hepatitis C virus RNA replication is regulated by host geranylgeranylation and fatty acids. Proc. Natl. Acad. Sci. U.S.A. 102, 2561–2566.

Kato, N., 2001. Molecular virology of hepatitis C virus. Acta Med. Okayama 55, 133–159.

Kato, N., Hijikata, M., Ootsuyama, Y., Nakagawa, M., Ohkoshi, S., Sugimura, T., Shimotohno, K., 1990. Molecular cloning of the human hepatitis C virus genome from Japanese patients with non-A, non-B hepatitis. Proc. Natl. Acad. Sci. U.S.A. 87, 9524–9528.

Kato, N., Sugiyama, K., Namba, K., Dansako, H., Nakamura, T., Takami, M., Naka, K., Nozaki, A., Shimotohno, K., 2003a. Establishment of a hepatitis C virus subgenomic replicon derived from human hepatocytes infected in vitro. Biochem. Biophys. Res. Commun. 306, 756–766.

Kato, T., Date, T., Miyamoto, M., Furusaka, A., Tokushige, K., Mizokami, M., Wakita, T., 2003b. Efficient replication of the genotype 2a hepatitis C virus subgenomic replicon. Gastroenterology 125, 1808–1817.

Kishine, H., Sugiyama, K., Hijikata, M., Kato, N., Takahashi, H., Noshi, T., Nio, Y., Hosaka, M., Miyanari, Y., Shimotohno, K., 2002. Subgenomic replicon derived from a cell line infected with the hepatitis C virus. Biochem. Biophys. Res. Commun. 293, 993–999.

Lohmann, V., Korner, F., Koch, J., Herian, U., Theilmann, L., Bartenschlager, R., 1999. Replication of subgenomic hepatitis C virus RNAs in a hepatoma cell line. Science 285, 110–113.

Marcello, T., Grakoui, A., Barba-Spaeth, G., Machlin, E.S., Kotenko, S.V., MacDonald, M.R., Rice, C.M., 2006. Interferons alpha and lambda inhibit hepatitis C virus replication with distinct signal transduction and gene regulation kinetics. Gastroenterology 131, 1887–1898.

Mori, K., Abe, K., Dansako, H., Ariumi, Y., Ikeda, M., Kato, N., 2008. New efficient replication system with hepatitis C virus genome derived from a patient with acute hepatitis C. Biochem. Biophys. Res. Commun. 371, 104–109.

Nakagawa, M., Sakamoto, N., Tanabe, Y., Koyama, T., Itsui, Y., Takeda, Y., Chen, C.H., Kakinuma, S., Oooka, S., Maekawa, S., Enomoto, N., Watanabe, M., 2005. Suppression of hepatitis C virus replication by cyclosporin a is mediated by blockade of cyclophilins. Gastroenterology 129, 1031–1041.

Pagliaccetti, N.E., Eduardo, R., Kleinstein, S.H., Mu, X.J., Bandi, P., Robek, M.D., 2008. Interleukin-29 functions cooperatively with interferon to induce antiviral gene expression and inhibit hepatitis C virus replication. J. Biol. Chem. 283, 30079–30089.

Pietschmann, T., Lohmann, V., Kaul, A., Krieger, N., Rinck, G., Rutter, G., Strand, D., Bartenschlager, R., 2002. Persistent and transient replication of full-length hepatitis C virus genomes in cell culture. J. Virol. 76, 4008–4021.

Robek, M.D., Boyd, B.S., Chisari, F.V., 2005. Lambda interferon inhibits hepatitis B and C virus replication. J. Virol. 79, 3851–3854.

Tanaka, T., Kato, N., Cho, M.J., Sugiyama, K., Shimotohno, K., 1996. Structure of the 3′ terminus of the hepatitis C virus genome. J. Virol. 70, 3307–3312.

Taylor, D.R., Shi, S.T., Romano, P.R., Barber, G.N., Lai, M.M.C., 1999. Inhibition of the interferon-inducible protein kinase PKR by HCV E2 protein. Science 285, 107–109.

Uze, G., Monneron, D., 2007. IL-28 and IL-29: newcomers to the interferon family. Biochimie 89, 729–734.

Wang, C., Gale Jr., M., Keller, B.C., Huang, H., Brown, M.S., Goldstein, J.L., Ye, J., 2005. Identification of FBL2 as a geranylgeranylated cellular protein required for hepatitis C virus RNA replication. Mol. Cell 18, 425–434.

Watashi, K., Hijikata, M., Hosaka, M., Yamaji, M., Shimotohno, K., 2003. Cyclosporin A suppresses replication of hepatitis C virus genome in cultured hepatocytes. Hepatology 38, 1282–1288.

Ye, J., Wang, C., Sumpter Jr., R., Brown, M.S., Goldstein, J.L., Gale Jr., M., 2003. Disruption of hepatitis C virus RNA replication through inhibition of host protein geranylgeranylation. Proc. Natl. Acad. Sci. U.S.A. 100, 15865–15870.

JOURNAL OF VIROLOGY, Mar. 2009, p. 2338–2348 Vol. 83, No. 5
0022-538X/09/$08.00+0 doi:10.1128/JVI.01840-08


# Arsenic Trioxide Inhibits Hepatitis C Virus RNA Replication through Modulation of the Glutathione Redox System and Oxidative Stress▽

Misao Kuroki,[1] Yasuo Ariumi,[1] Masanori Ikeda,[1] Hiromichi Dansako,[1] Takaji Wakita,[2] and Nobuyuki Kato[1]*

*Department of Tumor Virology, Okayama University Graduate School of Medicine, Dentistry, and Pharmaceutical Sciences, 2-5-1, Shikata-cho, Okayama 700-8558, Japan,[1] and Department of Virology II, National Institute of Infectious Diseases, 1-23-1 Toyama, Shinjuku-ku, Tokyo 162-8640, Japan[2]*

Received 2 September 2008/Accepted 13 December 2008

**Arsenic trioxide (ATO), a therapeutic reagent used for the treatment of acute promyelocytic leukemia, has recently been reported to increase human immunodeficiency virus type 1 infectivity. However, in this study, we have demonstrated that replication of genome-length hepatitis C virus (HCV) RNA (O strain of genotype 1b) was notably inhibited by ATO at submicromolar concentrations without cell toxicity. RNA replication of HCV-JFH1 (genotype 2a) and the release of core protein into the culture supernatants were also inhibited by ATO after the HCV infection. To clarify the mechanism of the anti-HCV activity of ATO, we examined whether or not PML is associated with this anti-HCV activity, since PML is known to be a target of ATO. Interestingly, we observed the cytoplasmic translocation of PML after treatment with ATO. However, ATO still inhibited the HCV RNA replication even in the PML knockdown cells, suggesting that PML is dispensable for the anti-HCV activity of ATO. In contrast, we found that *N*-acetyl-cysteine, an antioxidant and glutathione precursor, completely and partially eliminated the anti-HCV activity of ATO after 24 h and 72 h of treatment, respectively. In this context, it is worth noting that we found an elevation of intracellular superoxide anion radical, but not hydrogen peroxide, and the depletion of intracellular glutathione in the ATO-treated cells. Taken together, these findings suggest that ATO inhibits the HCV RNA replication through modulation of the glutathione redox system and oxidative stress.**

Hepatitis C virus (HCV) is the causative agent of chronic hepatitis, which progresses to liver cirrhosis and hepatocellular carcinoma. HCV is an enveloped virus with a positive single-stranded 9.6-kb RNA genome, which encodes a large polyprotein precursor of approximately 3,000 amino acid residues. This polyprotein is cleaved by a combination of the host and viral proteases into at least 10 proteins in the following order: core, envelope 1 (E1), E2, p7, nonstructural 2 (NS2), NS3, NS4A, NS4B, NS5A, and NS5B (30).

Alpha interferon has been used as an effective anti-HCV reagent in clinical therapy for patients with chronic hepatitis C. The current combination treatment with pegylated alpha interferon and ribavirin, a nucleoside analogue, has been shown to improve the sustained virological response rate to more than 50% (15). However, the adverse effects of the combination therapy and the limited efficacy against genotype 1b warrant the development of new anti-HCV reagents.

Arsenic trioxide (ATO) ($As_2O_3$, arsenite) has been used as a therapeutic reagent in acute promyelocytic leukemia, which bears an oncogenic PML-retinoic acid receptor alpha fusion protein resulting from chromosomal translocation (51, 52, 68, 70). The ATO treatment induces complete remission through degradation of the aberrant PML-retinoic acid receptor α (70). The PML tumor suppressor protein is required for formation of the PML nuclear body (PML-NB), also known as nuclear dot 10 or the PML oncogenic domain, which is often disrupted by infection with DNA viruses, such as herpes simplex virus type 1, human cytomegalovirus, and Epstein-Barr virus (17). The treatment with ATO results in degradation of the PML protein and disruption of the PML-NB (70). Therefore, ATO has been become a useful probe for investigating the functions of the PML-NB, including cell growth, apoptosis, stress response, and viral infection. Indeed, ATO has been shown to increase retroviral infectivity, such as human immunodeficiency virus type 1 (HIV-1) and murine leukemia virus infectivity, but the mechanisms of this change are not well understood (5, 6, 32, 44, 47, 50, 57). In contrast, ATO was recently reported to inhibit the replication of HCV subgenomic replicon RNA (24). However, it also remains unclear how ATO inhibits the HCV RNA replication. In this study, using genome-length HCV RNA replication systems, we investigated the molecular mechanism(s) of the anti-HCV activity of ATO, and we provide evidence that ATO inhibits HCV RNA replication through modulation of the glutathione redox system and oxidative stress.

## MATERIALS AND METHODS

**Reagents.** ATO, *N*-acetyl-cysteine (NAC), ascorbic acid (vitamin C), and L-buthionine sulfoximine (BSO) were purchased from Sigma (St. Louis, MO). Arsenic pentoxide (APO) ($As_2O_5$, arsenate) was purchased from Wako (Osaka, Japan). Both ATO and APO were dissolved in 1 N NaOH at 0.1 M as a stock solution. An inducible nitric oxide synthase (iNOS) inhibitor, 1400W, was purchased from Calbiochem (Merck Biosciences, Darmstadt, Germany).

**Cell culture.** 293FT cells were cultured in Dulbecco's modified Eagle's medium (Invitrogen, Carlsbad, CA, USA) supplemented with 10% fetal bovine serum. The following four HuH-7-derived cell lines or their parental HuH-7 cells

* Corresponding author. Mailing address: Department of Tumor Virology, Okayama University Graduate School of Medicine, Dentistry, and Pharmaceutical Sciences, 2-5-1, Shikata-cho, Okayama 700-8558, Japan. Phone: 81 86 235 7385. Fax: 81 86 235 7392. E-mail: nkato@md.okayama-u.ac.jp.

▽ Published ahead of print on 24 December 2008.

were cultured in Dulbecco's modified Eagle's medium with 10% fetal bovine serum as described previously (25): O cells, harboring a replicative genome-length HCV-O RNA (O strain of genotype 1b) (25); OR6 cells, harboring the genome-length HCV-O RNA with luciferase as a reporter (25); sO cells, harboring the subgenomic replicon RNA of HCV-O (31); and RSc cured cells, which cell culture-generated HCV-JFH1 (JFH1 strain of genotype 2a) (58) could infect and effectively replicate in (2, 3). The O, OR6, and sO cells were maintained in the presence of G418 (300 μg/ml Geneticin; Invitrogen).

**RNA interference.** Oligonucleotides with the following sense and antisense sequences were used for the cloning of short hairpin RNA (shRNA)-encoding sequences targeted to PML (56) in a lentiviral vector: 5′-GATCCCCAGATGC AGCTGTATCCAAGTTCAAGAGACTTGGATACAGCTGCATCTTTTTTG GAAA-3′ (sense) and 5′-AGCTTTTCCAAAAAAGATGCAGCTGTATCCAA GTCTCTTGAACTTGGATACAGCTGCATCTGGG-3′ (antisense). These oligonucleotides were annealed and subcloned into the BglII-HindIII site, downstream from an RNA polymerase III promoter of pSUPER (8), to generate pSUPER-PMLi. To construct pLV-PMLi, the BamHI-SalI fragments of pSUPER-PMLi were subcloned into the BamHI-SalI site of pRDI292, an HIV-1-derived self-inactivating lentiviral vector containing a puromycin resistance marker allowing for the selection of transduced cells (7). pLV-Chk2i was described previously (3).

**Lentiviral vector production.** The vesicular stomatitis virus (VSV) G-pseudotyped HIV-1-based vector system has been described previously (42). The lentiviral vector particles were produced by transient transfection of the second-generation packaging construct pCMV-ΔR8.91 (1, 71) and the VSV G envelope-expressing plasmid pMDG2 as well as pRDI292 into 293FT cells with FuGene6 (Roche Diagnostics, Mannheim, Germany).

**HCV infection experiments.** The supernatants was collected from cell culture-generated HCV-JFH1 (58)-infected RSc cells (2, 3) at 5 days postinfection and stored at −80°C after filtering through a 0.45-μm filter (Kurabo, Osaka, Japan) until use. For infection experiments with HCV-JFH1 virus, RSc cells ($1 \times 10^5$ cells/well) were plated onto six-well plates and cultured for 24 h. We then infected the cells with 50 μl (equivalent to a multiplicity of infection of 0.05 to 0.1) of inoculum. The culture supernatants were collected at 97 h postinfection, and the levels of the core protein were determined by enzyme-linked immunosorbent assay (Mitsubishi Kagaku Bio-Clinical Laboratories, Tokyo, Japan). Total RNA was isolated from the infected cellular lysates using an RNeasy minikit (Qiagen, Hilden, Germany) for quantitative reverse transcription-PCR (RT-PCR) analysis of intracellular HCV RNA. The level of intracellular HCV RNA in the RSc cells was $>10^8$ copies/μg total RNA at 4 days postinfection.

**Quantitative RT-PCR Analysis.** The quantitative RT-PCR analysis for HCV RNA was performed by real-time LightCycler PCR (Roche) as described previously (25). We used the following forward and reverse primer sets for the real-time LightCycler PCR: PML, 5′-GAGGAGTTCCAGTTTCTGCG-3′ (forward), 5′-GCGCCTGGCAGATGGGGCAC-3′ (reverse); β-actin, 5′-TGACGG GGTCACCCACACTG-3′ (forward), 5′-AAGCTGTAGCCGCGCTCGGT-3′ (reverse); HCV-O, 5′-AGAGCCATAGTGGTCTGCGG-3′ (forward), 5′-CTT TCGCGACCCAACACTAC-3′ (reverse); and HCV-JFH1, 5′-5′-AGAGCCAT AGTGGTCTGCGG-3′ (forward), 5′-CTTTCGCAACCCAACGCTAC-3′ (reverse).

**Western blot analysis.** Cells were lysed in buffer containing 50 mM Tris-HCl (pH 8.0), 150 mM NaCl, 4 mM EDTA, 1% Nonidet P-40, 0.1% sodium dodecyl sulfate, 1 mM dithiothreitol, and 1 mM phenylmethylsulfonyl fluoride. Supernatants from these lysates were subjected to sodium dodecyl sulfate-polyacrylamide gel electrophoresis, followed by immunoblot analysis using anti-PML (A301-168A-1; Bethyl Laboratories, Montgomery, TX), anti-Chk2 (DCS-273; Medical & Biological Laboratories, MBL, Nagoya, Japan), anti-HCV core (CP-9 and CP-11; Institute of Immunology, Tokyo, Japan), anti-HCV NS5A (no. 8926; a generous gift from A Takamizawa, The Research Foundation for Microbial Diseases of Osaka University, Japan), anti-signal transducer and activator of transcription 3 (anti-STAT3) (BD Bioscience, San Jose, CA), anti-phospho-STAT3 (Tyr705) (Cell Signaling Technology, Danvers, MA) anti-poly(ADP-ribose) polymerase 1 (anti-PARP-1) (C-2-10; Calbiochem), or anti-β-actin antibody (Sigma).

**MTT assay.** HuH-7 or O cells ($5 \times 10^3$ cells/well) were plated onto 96-well plates and cultured for 24 h. The cells were treated with ATO, APO, or NaOH for 24, 48, or 72 h and then subjected to the colorimetric 3-(4,5-dimethylthiazol-2-yl)-2,5-diphenyltetrazolium bromide (MTT) assay according to the manufacturer's instructions (cell proliferation kit I; Roche). The absorbance was read using a microplate reader (model 2550; Bio-Rad Laboratories, Hercules, CA) at 550 nm with a reference wavelength of 690 nm.

**RL assay.** OR6 cells ($1.5 \times 10^4$ cells/well) were plated onto 24-well plates and cultured for 24 h. The cells were treated with each reagent for 72 h and then subjected to the *Renilla* luciferase (RL) assay according to the manufacturer's instructions (Promega, Madison, WI). A Lumat LB9507 luminometer (Berthold, Bad Wildbad, Germany) was used to detect RL activity.

**FL assay.** Plasmids were transfected into O cells ($2 \times 10^4$ cells/well in 24-well plates) using FuGene6 and cultured for 24 h. The cells were treated with or without 1 μM ATO for 24 h, and then firefly luciferase (FL) assays were performed according to the manufacturer's instructions (Promega).

**Immunofluorescence and confocal microscopic analysis.** Cells were fixed in 3.6% formaldehyde in phosphate-buffered saline (PBS), permeabilized in 0.1% NP-40 in PBS at room temperature, and incubated with anti-PML antibody (PM001; MBL) at a 1:300 dilution in PBS containing 3% bovine serum albumin at 37°C for 30 min. They were then stained with fluorescein isothiocyanate-conjugated anti-rabbit antibody (Jackson ImmunoResearch, West Grove, PA) at a 1:300 dilution in PBS containing bovine serum albumin at 37°C for 30 min, followed by staining with 4′,6-diamidino-2-phenylindole (DAPI) at room temperature for 15 min. Following extensive washing in PBS, the cells were mounted on slides using a mounting medium of 90% glycerin–10% PBS with 0.01% *p*-phenylenediamine added to reduce fading. Samples were viewed under a confocal laser-scanning microscope (LSM510; Zeiss, Jena, Germany).

**Measurement of intracellular $O_2^-$ and $H_2O_2$ production.** The intracellular superoxide anion radical ($O_2^-$) levels were measured with an oxidation-sensitive fluorescent probe, dihydroethidium (DHE) (Invitrogen Molecular Probes), that is highly selective for detection of $O_2^-$ among reactive oxygen species (ROS). DHE is cell permeative and reacts with $O_2^-$ to form ethidium, which in turn intercalates in DNA, thereby exhibiting a red fluorescence. The intracellular hydrogen peroxide ($H_2O_2$) levels were measured with another oxidation-sensitive fluorescent probe dye, 6-carboxy-2′,7′-dichlorodihydrofluorescein diacetate (carboxy-$H_2$DCFDA) (Invitrogen Molecular Probes). Carboxy-$H_2$DCFDA was intracellularly deacetylated with esterase and further oxidized with peroxidase to the fluorescent 2′,7′-dichlorodihydrofluorescein (DCF). The ATO- or BSO-treated O cells were washed with PBS and incubated with 5 μM DHE and 20 μM carboxy-$H_2$DCFDA in PBS at 37°C for 30 min. Cells were then washed twice with PBS. The DHE or DCF fluorescence intensity was measured using a FACSCalibur flow cytometer. For each sample, 10,000 events were collected. The $O_2^-$ or $H_2O_2$ levels are indicated as mean fluorescence intensities, which were determined with the CellQuest software (BD Bioscience).

**Detection of intracellular glutathione.** Intracellular glutathione levels were analyzed using CellTracker Green (5-chloromethylfluorescein diacetate [CMFDA]; Molecular Probes, Invitrogen). CMFDA is a membrane-permeative dye used to determine intracellular glutathione levels. Cytoplasmic esterase converts the nonfluorescent CMFDA to the fluorescent 5-chloromethylfluorescein (CMF), which can then react with glutathione. The excitation peak is at 492 nm, and the fluorescence emission peak is at 517 nm. O cells treated with 1 μM ATO for 72 h were washed with PBS and incubated with 5 μM CMFDA at 37°C for 30 min. The CMF fluorescence intensity was measured using a FACSCalibur flow cytometer. For each sample, 10,000 events were collected. The glutathione levels are given as the relative mean fluorescence intensities, which were determined with CellQuest software.

## RESULTS

**ATO inhibits HCV RNA replication.** First, we quantitatively examined the effect of ATO on the HCV RNA replication in HuH-7-derived O cells harboring a replicative genome-length HCV-O RNA (25). We found that submicromolar concentrations of ATO markedly inhibited genome-length HCV-O RNA replication in the O cells at 72 h after administration (Fig. 1A). The 50% effective concentration ($EC_{50}$) of ATO required for inhibition of genome-length HCV-O RNA replication was 0.19 μM (Fig. 1A). Consistent with this finding, the expression levels of the HCV core and NS5A proteins were also significantly decreased in the cell lysates of O cells treated with ATO for 72 h (Fig. 1B). In addition, ATO markedly inhibited the replication of the subgenomic replicon RNA (31), with an $EC_{50}$ of 0.48 μM at 72 h after the treatment (Fig. 1C). We next examined the effect of ATO on HCV reproduction by HCV-JFH1 infection (58). The results revealed that ATO significantly inhibited the intracellular RNA replication of HCV-

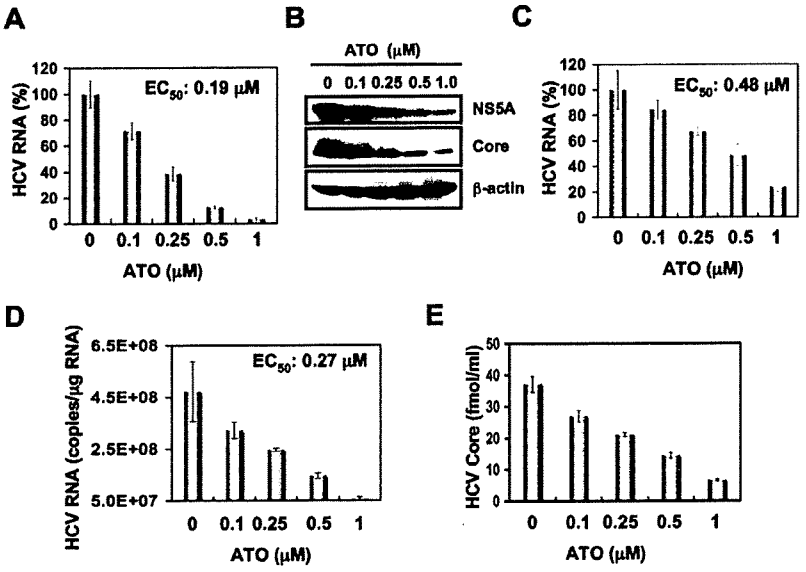


FIG. 1. Inhibition of HCV RNA replication by ATO. (A) The level of genome-length HCV RNA in O cells after the treatment with ATO was monitored by real-time LightCycler PCR. Experiments were done in triplicate and, bars represent the mean percentage of HCV RNA. Error bars indicate standard deviations. (B) HCV core and NS5A protein expression levels in O cells after treatment with ATO. The results of Western blot analysis of cellular lysates with anti-HCV core, anti-HCV NS5A, or anti-β-actin antibody in O cells at 72 h after treatment with ATO at the indicated concentration are shown. (C) The level of subgenomic replicon RNA was monitored by real-time LightCycler PCR. Results from three independent experiments conducted as described for panel A are shown. (D) The level of intracellular genome-length HCV-JFH1 RNA was monitored by real-time LightCycler PCR. RSc cells were pretreated with the indicated concentration of ATO for 13 h, followed by inoculation of the HCV-JFH1 virus, and then the infected cells were further incubated with ATO for 97 h. Results from three independent experiments conducted as described for panel A are shown. (E) The levels of the core protein in the culture supernatants treated as described for panel D were determined by enzyme-linked immunosorbent assay. Experiments were done in triplicate, and bars represent the mean core protein levels.

JFH1, with an $EC_{50}$ of 0.27 μM, as well as the release of core protein into the culture supernatants in HuH-7-derived RSc cells at 97 h after inoculation of the HCV-JFH1 virus (Fig. 1D and E). Thus, we have demonstrated for the first time that ATO can inhibit the reproduction of HCV and particularly HCV RNA replication.

**Effect of APO on HCV replication.** Arsenic is known to exist in two oxidation states, As(III) in ATO and As(V) in APO. As ATO in the lower valence state has been reported to be more toxic than APO (48), we compared their anti-HCV activities using an OR6 assay system, which was recently developed as a luciferase reporter assay system for monitoring genome-length HCV RNA replication in HuH-7-derived OR6 cells (Fig. 2A) (25). The results showed that APO could not strongly suppress HCV replication at submicromolar concentrations, while ATO strongly inhibited it, with an $EC_{50}$ of 0.33 μM (Fig. 2B and C), indicating that ATO has unique anti-HCV activity. In this context, it is relevant that the expression level of HCV core protein was also remarkably decreased in the cell lysates of O cells treated with ATO, but not those treated with APO, for 72 h (Fig. 2D). Thus, APO seems to be a useful negative probe to clarify the mechanism of the anti-HCV activity of ATO.

**ATO does not affect cell growth at submicromolar concentrations.** ATO has been reported to induce apoptosis (11, 14, 20, 21, 26–28, 33, 48, 66). Therefore, such an ATO-induced apoptosis may be involved in the anti-HCV activity. To test this possibility, we examined the effect of ATO or APO at various concentrations on cell proliferation by colorimetric MTT assay. In this context, we demonstrated that ATO did not affect the cell proliferation of O cells or the parental HCV-negative HuH-7 cells at submicromolar concentrations (Fig. 3A and E). In contrast, 4 or 8 μM ATO significantly inhibited cell proliferation (Fig. 3B and F). Similarly, APO did not affect the cell proliferation at less than 2 μM (Fig. 3C and D). Consistent with the above results, ATO-treated O cells exhibited normal growth rates and cell viabilities, at least at 1 μM for 72 h (Fig. 3G). Furthermore, we did not observe the cleavage of PARP-1, which is known to be an important substrate for activated caspase 3, in O cells treated with 1 μM ATO at least until 72 h (Fig. 3H), indicating that 1 μM ATO did not induce apoptosis in O cells. Thus, we concluded that the anti-HCV activity was independent of ATO-induced apoptosis or cell toxicity, at least at submicromolar concentrations.

**PML and Chk2 are dispensable for the anti-HCV activity of ATO.** Since PML is known to be a target of ATO (70), we first examined the subcellular localization of PML in O cells treated with either 1 μM ATO or 1 μM APO for 72 h by means of an anti-PML antibody (PM001; MBL) that can recognize most of the PML splicing variants and is useful for immunofluorescence analysis. The results showed that PML was localized predominantly in punctate nuclear speckles termed PML-NBs in control O cells (Fig. 4A). Interestingly, we noticed that some nuclear PML, but not all, disappeared and was translocated into discrete cytoplasmic bodies in the O cells treated with 1 μM ATO (Fig. 4A). We also observed cytoplasmic translocation of PML in the O cells treated with 1 μM APO for 72 h (Fig. 4A). Furthermore, we observed a similar cytoplasmic translocation of PML in the HCV-negative 293FT or HeLa

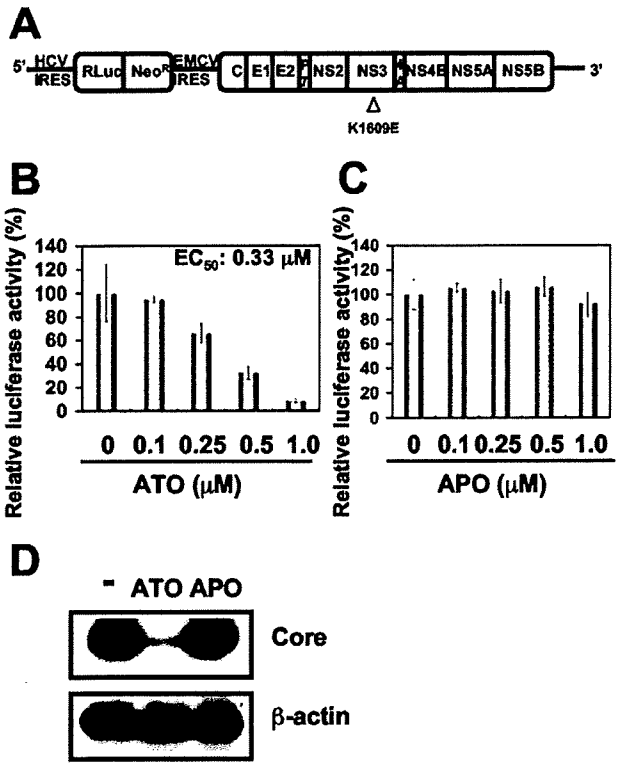


FIG. 2. Effect of APO on HCV replication. (A) Schematic representation of genome-length HCV RNA encoding the RL gene as a reporter (ORN/C-5B/KE RNA) replicated in OR6 cells. The RL is expressed as a fusion protein with neomycin phosphotransferase ($Neo^R$). The position of an adaptive mutation, K1609E in NS3, is indicated by an open triangle. (B) Effect of ATO on genome-length HCV RNA replication. At 72 h after treatment of OR6 cells with ATO at the indicated concentrations, the replication level of HCV RNA was monitored by the RL assay. The relative RL activity is shown. The results shown are means from three independent experiments. Error bars indicate standard deviations. (C) Effect of APO on genome-length HCV RNA replication. At 72 h after treatment of OR6 cells with APO at the indicated concentrations, the replication level of HCV RNA was monitored by the RL assay as described for panel B. (D) HCV core protein expression level in O cells after treatment with either ATO or APO. The results of Western blot analysis of cellular lysates with anti-HCV core or anti-β-actin antibody in O cells at 72 h after treatment with either 1 μM ATO or 1 μM APO are shown.

cells after the treatment with ATO (data not shown). Thus, we concluded that the cytoplasmic translocation of PML after the treatment with ATO was not associated with anti-HCV activity. Next, Western blot analysis to compare PML expression in the lysates of O cells treated with 1 μM ATO or 1 μM APO for 72 h was performed using another anti-PML antibody, A301-168A-1 (a gift from Bethyl Laboratories), which can recognize the longest isoform, PML I, but not shorter PML isoforms such as PML VI and which has been proven useful for Western blot analysis. Consistent with the previous finding that ATO promotes PML degradation (70), the expression level of the PML I protein was lower in the ATO-treated O cells than in the APO-treated O cells (Fig. 4B), suggesting that PML degradation by ATO is associated with anti-HCV activity. To further examine whether PML is directly involved in the anti-HCV activity of ATO, we used lentiviral vector-mediated RNA interference to stably knock down PML in the O cells. To express an shRNA targeted to all PML isoforms (56), we used the VSV G-pseudotyped HIV-1-based vector system (1, 42, 71). We used the puromycin-resistant pooled cells at 10 days after the lentiviral transduction in this experiment. Immunofluorescence and Western blot analysis demonstrated a very effective knockdown of PML in the O cells (Fig. 4C and D). We quantitatively examined the level of HCV RNA in the PML knockdown O cells treated with or without either 1 μM ATO (Fig. 4E) or 1 μM APO (Fig. 4F) for 72 h. The results showed that the replication level of genome-length HCV-O RNA in the untreated PML knockdown cells was similar to that in control cells (Fig. 4E), suggesting that PML is dispensable in HCV RNA replication. Importantly, ATO effectively inhibited the HCV RNA replication in both the PML knockdown cells and control cells compared with that of the APO-treated cells (Fig. 4E and F). Thus, we concluded that PML was dispensable for the anti-HCV activity of ATO. Since the Chk2 checkpoint kinase has recently been implicated in ATO-induced apoptosis and in association with PML (27, 63, 64, 66), we examined the anti-HCV activity in the ATO-treated Chk2 knockdown O cells (3). As we previously described, Western blot analysis demonstrated very effective knockdown of Chk2 in O cells (Fig. 4G). Accordingly, we examined the level of HCV RNA in Chk2 knockdown cells treated with or without either 1 μM ATO (Fig. 4H) or 1 μM APO (Fig. 4I) for 72 h. Consistent with our recent finding that Chk2 is required for HCV RNA replication, the replication of genome-length HCV RNA in the untreated Chk2 knockdown cells was remarkably suppressed (Fig. 4H). However, ATO strongly inhibited the HCV RNA replication in the Chk2 knockdown cells compared with that in the APO-treated Chk2 knockdown cells (Fig. 4H and I), suggesting that Chk2 is not implicated in the anti-HCV activity of ATO.

**Effect of ATO on the stress-signaling pathways.** To date, the focus has been on PML and PML-retinoic acid receptor α as major targets of ATO (70). On the other hand, arsenic has been reported to modulate other cell-signaling pathways, especially stress-responsive transcription factors, such as nuclear factor κB (NF-κB), activator protein 1 (AP-1), and STAT3 (12, 37, 38, 62). Therefore, we examined the involvement of several stress-responsive pathways in the anti-HCV activity of ATO by luciferase-based reporter assays or Western blot analysis using an antibody which specifically recognizes STAT3 phosphorylated at tyrosine 705. Although it has been reported that ATO inhibited the NF-κB signaling pathway through a direct interaction with IKKβ at a high concentration (more than 10 μM) (29), neither 1 μM ATO nor 1 μM APO affected the endogenous NF-κB transcriptional activity in the present study (Fig. 5A and B). Conversely, ATO at least slightly stimulated mitogen-activated protein kinase kinase kinase (MEKK)-mediated NF-κB activation (Fig. 5A and B). Since NF-κB activation has been shown to stimulate HCV replication (60), the NF-κB pathway would seem not to be essential for the anti-HCV activity of ATO. Next, regarding the AP-1 signaling pathway, both ATO and APO are known to activate c-Jun N-terminal kinase (JNK) (45). Importantly, there was no stimulation of JNK activity at a dose below 30 μM (45). In fact, 50 μM ATO but not 50 μM APO strongly stimulates AP-1 activity by in-

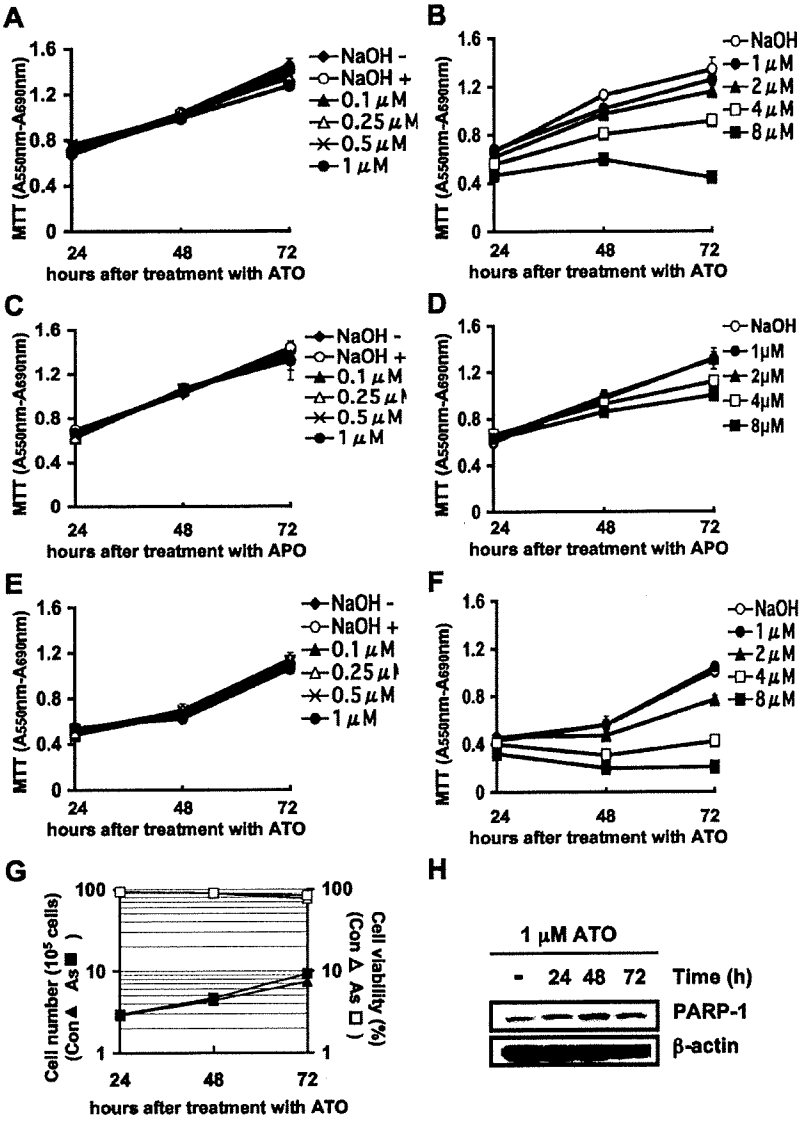


FIG. 3. Effect of ATO on cell growth and viability. (A and B) MTT assay of O cell lysates at the indicated times after treatment with ATO at various concentrations. NaOH (10 μM) was used as the solvent for ATO. The results shown are means from three independent experiments. Error bars indicate standard deviations. (C and D) MTT assay of O cell lysates at the indicated times after treatment with APO at various concentrations. (E and F) MTT assay of HuH-7 cell lysates at the indicated times after treatment with ATO at various concentrations. (G) Growth curve and viability of O cells after treatment with either 10 μM NaOH (Con) or 1 μM ATO (As). (H) Western blot analysis of cellular lysates with anti-PARP-1 or anti-β-actin antibody in O cells at the indicated times after treatment with 1 μM ATO.

hibiting a JNK phosphatase (10). Consistently, we found that both 1 μM ATO and 1 μM APO had a marginal effect on the AP-1 signaling pathway (Fig. 5C and D), suggesting that the AP-1 pathway is also not involved in the anti-HCV activity of ATO. Regarding the STAT3 signaling pathway, ATO has been reported to inhibit the phosphorylation of the STAT3 tyrosine at 705, leading to inactivation of the JAK-STAT signaling pathway (12, 62). In contrast, it has been reported that HCV constitutively phosphorylates and activates STAT3 (49, 59, 67). In this context, we observed constitutive tyrosine phosphorylation of STAT3 in untreated O cells (Fig. 5E). Furthermore, the marginal effect of 1 μM ATO on STAT3 phosphorylation and interleukin-6-mediated STAT3 activation was also observed (Fig. 5E and F). Taken together, these results at least suggest that the NF-κB, AP-1, and STAT3 pathways may not be associated with the anti-HCV activity of ATO at submicromolar concentrations.

**The anti-HCV activity of ATO is associated with the glutathione redox system and oxidative stress.** Finally, we focused on the involvement of the glutathione redox system and oxidative stress in the anti-HCV activity of ATO. For this, we analyzed the HCV replication level after combination treatment with ATO and antioxidants such as NAC and vitamin C using the OR6 assay system. When OR6 cells were treated with

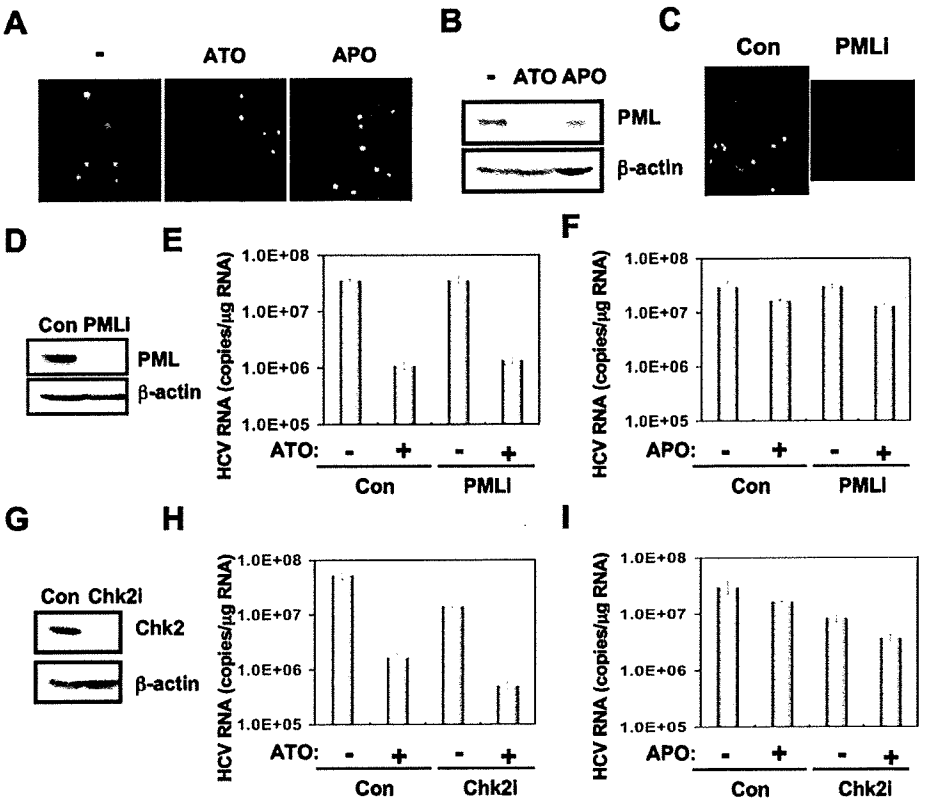


FIG. 4. PML and Chk2 are not required for the anti-HCV activity of ATO. (A) Subcellular localization of PML in O cells at 72 h after treatment with 10 μM NaOH (−), 1 μM ATO, or 1 μM APO. PML was detected by indirect immunofluorescence analysis with anti-PML antibody (PM001). DAPI staining of the nuclear DNA is also shown. (B) Induction of PML degradation by ATO but not by APO. The results of Western blot analysis of cellular lysates of O cells at 72 h after treatment with 10 μM NaOH (−), 1 μM ATO, or 1 μM APO with anti-PML (A301-168A-1) or anti-β-actin antibody are shown. (C) Stable knockdown of PML by shRNA-producing lentiviral vector in O cells. PML was detected by indirect immunofluorescence analysis with anti-PML antibody (PM001) in O cells expressing shRNA targeted to PML (PMLi) as well as in O cells transduced with a control lentiviral vector (Con). (D) Western blot analysis of cellular lysates with anti-PML (A301-168A-1) or anti-β-actin antibody in PML knockdown O cells (PMLi) as well as in control O cells (Con). (E and F) The level of genome-length HCV-O RNA was monitored by real-time LightCycler PCR in PML knockdown O cells (PMLi) as well as in control O cells (Con) after treatment with 10 μM NaOH (−), 1 μM ATO (+) (E), or 1 μM APO (+) (F) for 72 h. Results from three independent experiments conducted as described in the legend to Fig. 1A are shown. (G) Inhibition of Chk2 expression by shRNA-producing lentiviral vector. The results of Western blot analysis of cellular lysates with anti-Chk2 or anti-β-actin antibody in O cells expressing shRNA targeted to Chk2 (Chk2i) as well as in O cells transduced with a control lentiviral vector (Con) are shown. (H and I) The level of genome-length HCV-O RNA was monitored by real-time LightCycler PCR in Chk2 knockdown O cells (Chk2i) as well as in control O cells (Con) after treatment with 10 μM NaOH (−), 1 μM ATO (+) (H), or 1 μM APO (+) (I) for 72 h. Results from three independent experiments conducted as described in the legend to Fig. 1A are shown.

either 100 μM vitamin C or 10 mM NAC alone for 24 h or 72 h, the HCV replication was slightly enhanced (Fig. 6A and B), indicating that the antioxidant can activate HCV replication. Although the anti-HCV activity in the OR6 cells treated with 1 μM ATO and in combination with 100 μM vitamin C for 24 h was weakly reduced, 10 mM NAC completely and partially eliminated the anti-HCV activity of ATO after 24 h (Fig. 6A) and 72 h (Fig. 6B) of treatment, respectively, suggesting that oxidative stress and the glutathione redox system are associated with the anti-HCV activity of ATO. In contrast, the iNOS inhibitor 1400W did not suppress the HCV RNA replication or eliminate the anti-HCV activity of ATO, suggesting that NO is not involved in the anti-HCV activity of ATO (Fig. 6C). To further examine the involvement of oxidative stress in the anti-HCV activity of ATO, we examined ROS production in ATO-treated cells using two oxidative-sensitive fluorescent probes, DHE for detection of intracellular $O_2^-$ and DCF for detection of intracellular $H_2O_2$. We found that 1 μM ATO could generate a significant level of intracellular $O_2^-$ but not intracellular $H_2O_2$, while 2 μM BSO, an inhibitor of glutathione synthesis (14, 20, 33), could induce both $O_2^-$ and $H_2O_2$ (Fig. 6D to H). Importantly, NAC diminished the ATO-dependent $O_2^-$ induction (Fig. 6F). Since glutathione is a major antioxidant in cells and can clear away superoxide anion free radical, we also analyzed the changes of the intracellular glutathione level in ATO-treated O cells using CMF fluorescence, which can react with glutathione. As a result, we observed significant glutathione depletion in the cells treated with at least 1 μM ATO (Fig. 6I). To further confirm the involvement of glutathione in the anti-HCV activity of ATO, we examined the effect of cotreatment with ATO and BSO. When the OR6 cells were treated with 1 μM BSO alone, the HCV replication

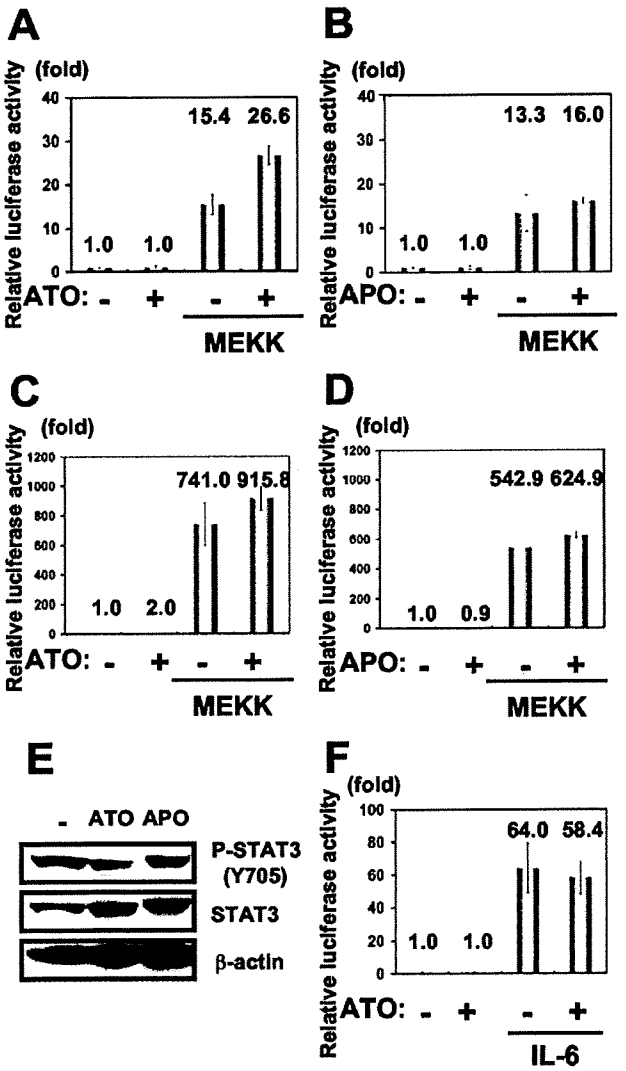


FIG. 5. Effect of ATO on the stress-signaling pathways. (A and B) Effect of ATO or APO on the NF-κB signaling pathway. O cells were transfected with 100 ng of reporter plasmid, pNF-κB-Luc, and/or 100 ng of pFC-MEKK (Stratagene, La Jolla, CA). Cells were treated with either 1 μM ATO (A) or 1 μM APO (B), and an FL assay was performed 24 h later. The results shown are means from three independent experiments. The relative FL activity is shown. (C and D) Effect of ATO or APO on the AP-1 signaling pathway. O cells were transfected with 100 ng of pAP-1-Luc and/or 100 ng of pFC-MEKK (Stratagene). Cells were treated with either 1 μM ATO (C) or 1 μM APO (D), and an FL assay was performed 24 h later as described for panels A and B. (E) Effect of ATO on the phosphorylation level of STAT3 at tyrosine 705. The results of Western blot analysis of cellular lysates with anti-phospho-STAT3 (Tyr705), anti-STAT3, or anti-β-actin antibody in O cells treated with either 1 μM ATO or 1 μM APO for 24 h are shown. (F) Effect of ATO on the STAT3 signaling pathway. O cells were transfected with 100 ng of STAT3 reporter APRE-Luc (41) (STAT3-Luc, a generous gift from T. Hirano, Osaka University, Japan). Cells were treated with 1 μM ATO for 19 h and then stimulated with 100 ng/ml of interleukin-6 for 5 h, and an FL assay was performed as described for panels A and B.

level was suppressed by about 30% compared with that of the control cells, and this occurred without cell toxicity (data not shown). However, consistent with previous reports in which ATO-induced apoptosis was enhanced by BSO (14, 20, 33), most of the cells died, possibly through apoptosis, when the OR6 cells were cotreated with 1 μM ATO and 1 μM BSO for 72 h (data not shown), suggesting that ATO and BSO synergistically generate ROS and deplete glutathione, resulting in induction of oxidative damage. Taken together, these results suggest that ATO may inhibit the HCV RNA replication by modulating the glutathione redox system and oxidative stress.

## DISCUSSION

ATO has been reported to affect multiple biological functions, such as PML-NB formation, apoptosis, differentiation, stress response, and viral infection (38). Indeed, ATO has been shown to increase retroviral infectivity, including infectivity of HIV-1, HIV-2, feline immunodeficiency virus, simian immunodeficiency virus from rhesus macaques, and murine leukemia virus, although the mechanisms responsible for these changes are not well understood (5, 6, 32, 44, 47, 50, 57). PML, which is involved in host antiviral defenses, is required for the formation of the PML-NB, which is often disrupted or sequestered in the cytoplasm by infection with DNA or RNA viruses (17). The fact that ATO promotes the degradation of PML and alters the morphology or distribution of PML-NBs suggests that ATO enhances HIV-1 infection by antagonizing an antiviral activity associated with PML. In fact, HIV-1 infection has been reported to alter PML localization (57), although others have failed to confirm this finding (5). Furthermore, Berthoux et al. demonstrated that ATO stimulated retroviral reverse transcription (5). Moreover, ATO has been shown to have an inhibitory effect on host restriction factors, such as TRIM5a, Refl, and Lv1, in a cell type-dependent manner (5, 6, 32, 44, 47, 50). In contrast, we have demonstrated that ATO strongly inhibited genome-length HCV RNA replication without cell toxicity (Fig. 1A and 2A). In addition, we observed the cytoplasmic translocation of PML in the HCV RNA-replicating O cells after the treatment with ATO (Fig. 4A). However, PML was dispensable for the anti-HCV activity of ATO as well as HCV RNA replication (Fig. 4E). In this regard, it is worth noting the recent report by Herzer et al. that the HCV core protein interacts with PML isoform IV and abrogates the PML function (22). Thus, PML may be involved in the HCV life cycle. In any case, the sensitivity to ATO and the cellular target of ATO seem to be different between HCV and HIV-1.

HCV infection has been shown to cause a state of chronic oxidative stress like that seen in chronic hepatitis C, which may contribute to fibrosis and carcinogenesis in the liver (16, 18, 40). In particular, HCV replication has been associated with the endoplasmic reticulum (ER), where HCV causes ER stress. Indeed, HCV NS5A and core, the ER-associated proteins, have been reported to trigger ER stress (4, 55). Therefore, HCV infection causes production of ROS and lowering of mitochondrial transmembrane potential through calcium signaling (4, 36). Among the HCV proteins, core, E1, NS3, and NS5A have been shown to be potent ROS inducers, and these HCV proteins also alter intracellular calcium levels and induce oxidative stress, thereby inducing DNA damage, and constitu-

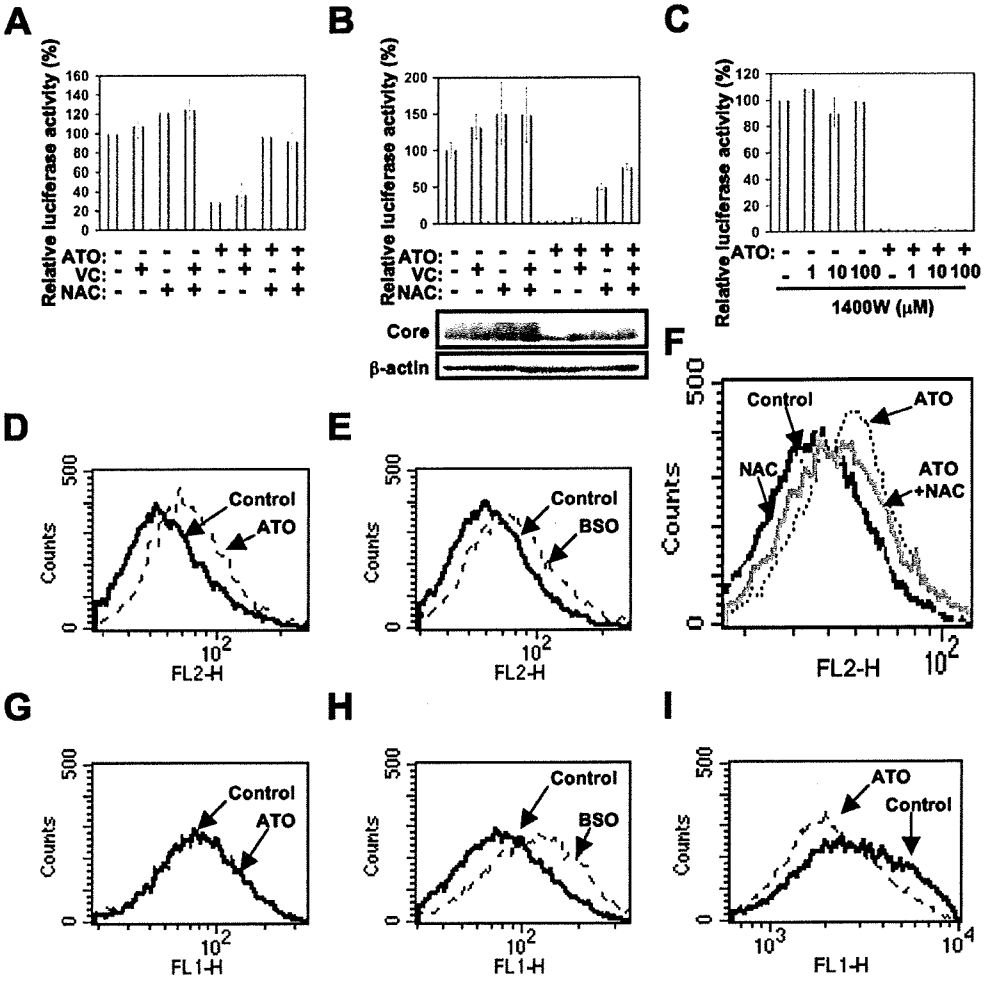


FIG. 6. The anti-HCV activity of ATO is associated with the glutathione redox system and oxidative stress. (A and B) The anti-HCV activity of ATO is eliminated by treatment with the antioxidant NAC. OR6 cells were treated with 1 μM ATO alone and in combination with 100 μM vitamin C (VC), with or without 10 mM NAC, for 24 h (A) or 72 h (B). The replication level of HCV RNA was monitored by the RL assay. The relative RL activity is shown. The results shown are means from three independent experiments; error bars indicate standard deviations. The results of Western blot analysis of cellular lysates with anti-HCV core or anti-β-actin antibody in OR6 cells at 72 h after the treatment with 1 μM ATO alone and in combination with 100 μM VC, with or without 10 mM NAC, are also shown. (C) Effect of combination treatment with ATO and the iNOS inhibitor 1400W on HCV RNA replication. OR6 cells were treated with 1 μM ATO alone and in combination with 1400W at the indicated concentrations for 72 h. The replication level of HCV RNA was monitored by the RL assay as described for panels A and B. (D and E) Effect of ATO on production of a ROS, $O_2^-$, in O cells. O cells were treated with 1 μM ATO (D) or 2 μM BSO (E) for 24 h. The intracellular $O_2^-$ level was measured by flow cytometry using DHE as described in Materials and Methods. (F) Inhibition of ATO-dependent $O_2^-$ induction by NAC. O cells were treated with either 1 μM ATO or 10 mM NAC alone and in combination with 10 mM NAC for 24 h. (G and H) Effect of ATO on production of a ROS, $H_2O_2$, in O cells. O cells were treated with 1 μM ATO (G) or 2 μM BSO (H) for 24 h. The intracellular $H_2O_2$ level was measured by flow cytometry using DCF as described in Materials and Methods. (I) Effect of ATO on the intracellular glutathione level in O cells. O cells were treated with 1 μM ATO for 72 h. The intracellular glutathione level was measured by flow cytometry using CellTracker Green CMFDA as described in Materials and Methods.

tively activate STAT3 and NF-κB, which are associated with HCV pathogenesis (19, 34, 36, 43, 49, 59, 60, 67). In fact, oxidative stress has been shown to trigger STAT3 tyrosine phosphorylation and nuclear translocation, which correlate with the activation of STAT3, leading to its DNA-binding activity (9). In contrast, ATO inhibited the STAT3 tyrosine phosphorylation through direct interaction with JAK kinase, thereby suppressing the transcriptional activity of STAT3 (12, 62). Importantly, STAT3 activation has been reported to be associated with HCV RNA replication (59, 69). The STAT3 Tyr705 dominant negative mutant has been shown to inhibit HCV RNA replication, suggesting that STAT3 positively regulates HCV replication (59). In contrast, others have reported that STAT3 induces anti-HCV activity (69). In this study, we analyzed the potential effect of ATO treatment on a set of stress-signaling events, including the NF-κB, AP-1, and STAT3 pathways, since ATO is known to modulate various signaling pathways. However, at 1 μM, which exerted an anti-HCV activity, the respective signaling pathways were not affected, arguing that the anti-HCV activity is independent of these

pathways (Fig. 5). In this regard, these stress-signaling pathways have been reported to be constitutively activated in HCV core- or NS5A-expressing cells (19, 36, 49, 59, 60, 67). In addition, previous studies demonstrated that ATO modulates the NF-κB, AP-1, and STAT3 pathways at higher concentrations (NF-κB, >10 μM; AP-1, >30 μM; STAT3, >4 μM). Therefore, we may have only observed the marginal effect of ATO in this study (Fig. 5). On the other hand, the HCV core or NS3 protein as well as HCV infection induces NO, leading to induction of double-stranded DNA breaks and accumulation of mutations of cellular genes (35). However, the iNOS inhibitor 1400W could not suppress HCV RNA replication and the anti-HCV activity of ATO, indicating that NO is not associated with the anti-HCV activity or with HCV replication (Fig. 6C).

It has been indicated that oxidative damage plays an important role in the effect of ATO (38). ROS generated in response to ATO exposure lead to accumulation of intracellular $H_2O_2$. Glutathione peroxidase and catalase are key enzymes regulating the levels of ROS and protecting cells from ATO-induced damage (26). However, the gastrointestinal glutathione peroxidase was drastically downregulated in cells harboring HCV replicons, which are rendered more susceptible to oxidative stress (39). The glutathione redox system has been implicated in the cellular defense system (14, 20). Glutathione, a major antioxidant in cells, is a tripeptide synthesized from cysteine, glutamic acid, and glycine, and it can scavenge superoxide anion free radicals. ATO has been shown to bind to the sulfhydryl group of glutathione and deplete the intracellular glutathione, resulting in enhancement of the sensitivity to oxidative damage (20, 33). Conversely, the antioxidant NAC is readily taken up by cells and serves as a precursor to elevate intracellular glutathione (53). In fact, ATO-induced apoptosis has been shown to be inhibited by NAC (11, 14, 21, 28). In this study, we have demonstrated that the anti-HCV activity of ATO was completely eliminated by treatment with NAC for 24 h (Fig. 6A). In addition, we found that ATO increased intracellular $O_2^-$ but not $H_2O_2$ and depleted the intracellular glutathione in HCV RNA-replicating cells (Fig. 6D to I). Importantly, NAC diminished the ATO-dependent $O_2^-$ induction (Fig. 6F). This finding could strengthen the link between ATO-dependent oxidative stress and anti-HCV activity. Similarly, Wen et al. reported an increase in ROS and enhanced susceptibility to glutathione depletion in the HCV core-expressing HepG2 cells (61). Accordingly, ROS have been shown to significantly suppress RNA replication in HCV replicon-harboring cells treated with $H_2O_2$ (13). In addition, HCV replication has been shown to be inhibited by lipid peroxidation of arachidonate, and this peroxidation could be blocked by lipid-soluble antioxidants such as vitamin E (23). Conversely, several antioxidants, such as vitamin C, vitamin E, and NAC, enhanced HCV replication in the present study (Fig. 6A and B) (65). Thus, we suggest that ATO inhibited HCV RNA replication by modulating the glutathione redox system and oxidative stress. In contrast to the above findings with HCV, NAC has been shown to suppress HIV-1 replication by preventing the activation of HIV-1 long terminal repeat transcription by NF-κB, suggesting a correlation between a decrease in glutathione levels and activation of HIV-1 replication (46, 53, 54). In this context, ATO has shown opposite effects on HIV-1 and HCV replication, stimulating the former and inhibiting the latter. Considering all of these results together, ATO can be regarded as a useful, novel anti-HCV reagent. In addition, the host redox system may be critical for HCV replication and may represent a pivotal target for the clinical treatment of patients with chronic hepatitis C.

## ACKNOWLEDGMENTS

We thank D. Trono, R. Agami, R. Iggo, A. Takamizawa, T. Hirano, A. Yoshimura, and M. Hijikata for the VSV G-pseudotyped HIV-1-based vector system pCMVΔR8.91, pMDG2, pSUPER, pRDI292, anti-NS5A antibody, APRE-Luc, and 293FT cells. We also thank T. Stamminger, M. Yano, and T. Nakamura for their helpful suggestions and technical assistance.

This work was supported by a Grant-in-Aid for Scientific Research (C) from the Japan Society for the Promotion of Science (JSPS); by a Grant-in-Aid for Research on Hepatitis from the Ministry of Health, Labor, and Welfare of Japan; by the Kawasaki Foundation for Medical Science and Medical Welfare; by the Okayama Medical Foundation; and by the Ryobi Teien Memorial Foundation.

## REFERENCES

1. **Ariumi, Y., T. Priscilla, M. Masutani, and D. Trono.** 2005. DNA damage sensors ATM, ATR, DNA-PKcs, and PARP-1 are dispensable for human immunodeficiency virus type 1 integration. J. Virol. **79**:2973–2978.
2. **Ariumi, Y., M. Kuroki, K. Abe, H. Dansako, M. Ikeda, T. Wakita, and N. Kato.** 2007. DDX3 DEAD-box RNA helicase is required for hepatitis C virus RNA replication. J. Virol. **81**:13922–13926.
3. **Ariumi, Y., M. Kuroki, H. Dansako, K. Abe, M. Ikeda, T. Wakita, and N. Kato.** 2008. The DNA damage sensors, ataxia-telangiectasia mutated kinase and checkpoint kinase 2 are required for hepatitis C virus RNA replication. J. Virol. **82**:9639–9646.
4. **Benali-Furet, N. L., M. Chami, L. Houel, F. De Giorgi, F. Vernejoul, D. Lagorce, L. Buscail, R. Bartenschlager, F. Ichas, R. Rizzuto, and P. Paterlini-Bréchot.** 2005. Hepatitis C virus core triggers apoptosis in liver cells by inducing ER stress and ER calcium depletion. Oncogene **24**:4921–4933.
5. **Berthoux, L., G. J. Towers, C. Gurer, P. Salomoni, P. P. Pandolfi, and J. Luban.** 2003. As2O3 enhances retroviral reverse transcription and counteracts Ref1 antiviral activity. J. Virol. **77**:3167–3180.
6. **Berthoux, L., S. Sebastian, E. Sokolskaja, and J. Luban.** 2004. Lv1 inhibition of human immunodeficiency virus type 1 is counteracted by factors that stimulate synthesis or nuclear translocation of viral cDNA. J. Virol. **78**: 11739–11750.
7. **Bridge, A. J., S. Pebernard, A. Ducraux, A. L. Nicoulaz, and R. Iggo.** 2003. Induction of an interferon response by RNAi vectors in mammalian cells. Nat. Genet. **34**:263–264.
8. **Brummelkamp, T. R., R. Bernard, and R. Agami.** 2002. A system for stable expression of short interfering RNAs in mammalian cells. Science **296**:550–553.
9. **Carballo, M., M. Conde, R. E. Bekay, J. Martín-Nieto, M. J. Camacho, J. Monteseirín, J. Conde, F. J. Bedoya, and F. Sobrino.** 1999. Oxidative stress triggers STAT3 tyrosine phosphorylation and nuclear translocation in human lymphocytes. J. Biol. Chem. **274**:17580–17586.
10. **Cavigelli, M., W. W. Li, A. Lin, B. Su, K. Yoshioka, and M. Karin.** 1996. The tumor promoter arsenite stimulates AP-1 activity by inhibiting a JNK phosphatase. EMBO J. **15**:6269–6279.
11. **Chen, Y. C., S. Y. Lin-Shiau, and J. K. Lin.** 1998. Involvement of reactive oxygen species and caspase 3 activation in arsenite-induced apoptosis. J. Cell Physiol. **177**:324–333.
12. **Cheng, H. Y., P. Li, M. David, T. E. Smithgall, L. Feng, and M. W. Lieberman.** 2004. Arsenic inhibition of the JAK-STAT pathway. Oncogene **23**: 3603–3612.
13. **Choi, J., K. J. Lee, Y. Zheng, A. K. Yamaga, M. M. C. Lai, and J. H. Ou.** 2004. Reactive oxygen species suppress hepatitis C virus RNA replication in human hepatoma cells. Hepatology **39**:81–89.
14. **Dai, J., R. S. Weinberg, S. Waxman, and Y. Jing.** 1999. Malignant cells can be sensitized to undergo growth inhibition and apoptosis by arsenic trioxide through modulation of the glutathione redox system. Blood **93**:268–277.
15. **Davis, G. L.** 2006. Tailoring antiviral therapy in hepatitis C. Hepatology **43**:909–911.
16. **De Maria, N., A. Colantoni, S. Fagiuoli, G. J. Liu, B. K. Rogers, F. Farinati, D. H. Van Thiel, and R. A. Floyd.** 1996. Association between reactive oxygen species and disease activity in chronic hepatitis C. Free Radic. Biol. Med. **21**:291–295.
17. **Everett, R. D., and M. K. Chelbi-Alix.** 2007. PML and PML nuclear bodies: implications in antiviral defence. Biochemie **89**:819–830.
18. **Farinati, F., R. Cardin, N. De Maria, G. D. Libera, C. Marafin, E. Lecis, P.**

**Burra, A. Floreani, A. Cecchetto, and R. Naccarato.** 1995. Iron storage, lipid peroxidation and glutathione turnover in chronic anti-HCV positive hepatitis. J. Hepatol. **22**:449–456.
19. **Gong, G., G. Waris, R. Tanveer, and A. Siddiqui.** 2001. Human hepatitis C virus NS5A protein alters intracellular calcium levels, induces oxidative stress, and activates STAT-3 and NF-κB. Proc. Natl. Acad. Sci. USA **98**: 9599–9604.
20. **Han, Y. H., S. H. Kim, S. Z. Kim, and W. H. Park.** 2008. Apoptosis in arsenic trioxide-treated Calu-6 lung cells is correlated with the depletion of GSH levels rather than the change of ROS levels. J. Cell. Biochem. **104**:862–878.
21. **Han, Y. H., S. Z. Kim, S. H. Kim, and W. H. Park.** 2008. Suppression of arsenic trioxide-induced apoptosis in HeLa cells by N-acetylcysteine. Molecules Cells **26**:18–25.
22. **Herzer, K., S. Weyer, P. H. Krammer, P. R. Galle, and T. G. Hofmann.** 2005. Hepatitis C virus core protein inhibits tumor suppressor protein promyelocytic leukemia function in human hepatoma cells. Cancer Res. **65**:10830–10837.
23. **Huang, H., Y. Chen, and J. Ye.** 2007. Inhibition of hepatitis C virus replication by peroxidation of arachidonate and restoration by vitamin E. Proc. Natl. Acad. Sci. USA **104**:18666–18670.
24. **Hwang, D. R., Y. C. Tsai, J. C. Lee, K. K. Huang, R. K. Lin, C. H. Ho, J. M. Chiou, Y. T. Lin, J. T. A. Hsu, and C. T. Yeh.** 2004. Inhibition of hepatitis C virus replication by arsenic trioxide. Antimicrob. Agents Chemother. **48**: 2876–2882.
25. **Ikeda, M., K. Abe, H. Dansako, T. Nakamura, K. Naka, and N. Kato.** 2005. Efficient replication of a full-length hepatitis C virus genome, strain O, in cell culture, and development of a luciferase reporter system. Biochem. Biophys. Res. Commun. **329**:1350–1359.
26. **Jing, Y., J. Dai, R. M. E. Chalmers-Redman, W. G. Tatton, and S. Waxman.** 1999. Arsenic trioxide selectively induces acute promyelocytic leukemia cell apoptosis via a hydrogen peroxide-depndent pathway. Blood **94**:2102–2111.
27. **Joe, Y., J. H. Jeong, S. Yang, H. Kang, N. Motoyama, P. P. Pandolfi, J. H. Chung, and M. K. Kim.** 2006. ATR, PML, and Chk2 play a role in arsenic trioxide-induced apoptosis. J. Biol. Chem. **281**:28764–28771.
28. **Kang, Y. H., M. J. Yi, M. J. Kim, M. T. Park, S. Bae, C. M. Kang, C. K. Cho, I. C. Park, M. J. Park, C. H. Rhee, S. I. Hong, H. Y. Chung, Y. S. Lee, and S. J. Lee.** 2004. Caspase-independent cell death by arsenic trioxide in human cervical cancer cells: reactive oxygen species-mediated poly(ADP-ribose) polymerase-1 activation signals apoptosis-inducing factor release from mitochondria. Cancer Res. **64**:8960–8967.
29. **Kapahi, P., T. Takahashi, G. Natoli, S. R. Adams, Y. Chen, R. Y. Tsien, and M. Karin.** 2000. Inhibition of NF-κB activation by arsenite through reaction with a critical cysteine in the activation loop of IκB kinase. J. Biol. Chem. **275**:36062–36066.
30. **Kato, N.** 2001. Molecular virology of hepatitis C virus. Acta Med. Okayama **55**:133–159.
31. **Kato, N., K. Sugiyama, K. Namba, H. Dansako, T. Nakamura, M. Takami, K. Naka, A. Nozaki, and K. Shimotohno.** 2003. Establishment of a hepatitis C virus subgenomic replicon derived from human hepatocytes infected in vitro. Biochem. Biophys. Res. Commun. **306**:756–766.
32. **Keckesova, Z., L. M. J. Ylinen, and G. J. Towers.** 2004. The human and African green monkey TRIM5α genes encode Ref1 and Lv1 retroviral restriction factor activities. Proc. Natl. Acad. Sci. USA **101**:10780–10785.
33. **Kito, M., Y. Akao, N. Ohishi, K. Yagi, and Y. Nozawa.** 2002. Arsenic trioxide-induced apoptosis and its enhancement by buthionine sulfoximine in hepatocellular carcinoma cell lines. Biochem. Biophys. Res. Commun. **291**:861–867.
34. **Korenaga, M., T. Wang, Y. Li, L. A. Showalter, T. Chan, J. Sun, and S. A. Weinman.** 2005. Hepatitis C virus core protein inhibits mitochondrial electron transport and increases reactive oxygen species (ROS) production. J. Biol. Chem. **280**:37481–37488.
35. **Machida, K., K. T. Cheng, V. M. Sung, K. J. Lee, A. M. Levine, and M. M. C. Lai.** 2004. Hepatitis C virus infection activates the immunologic (type II) isoform of nitric oxide synthase and thereby enhances DNA damage and mutations of cellular genes. J. Virol. **78**:8835–8843.
36. **Machida, K., K. T. H. Cheng, C. K. Lai, K. S. Jeng, V. M. H. Sung, and M. M. C. Lai.** 2006. Hepatitis C virus triggers mitochondrial permeability transition with production of ractive oxygen species, leading to DNA damage and STAT3 activation. J. Virol. **80**:7199–7207.
37. **Meyer, M., R. Schreck, and P. A. Baeuerle.** 1993. $H_2O_2$ and antioxidants have opposite effects on activation of NF-κB and AP-1 in intact cells: AP-1 as secondary antioxidant-responsive factor. EMBO J. **12**:2005–2015.
38. **Miller, W. H., Jr., H. M. Schipper, J. S. Lee, J. Singer, and S. Waxman.** 2002. Mechanisms of action of arsenic trioxide. Cancer Res. **62**:3893–3903.
39. **Morbitzer, M., and T. Herget.** 2005. Expression of gastrointestinal glutathione peroxidase is inversely correlated to the presence of hepatitis C virus subgenomic RNA in human liver cells. J. Biol. Chem. **280**:8831–8841.
40. **Moriya, K., K. Nakagawa, T. Santa, Y. Shintani, H. Fujie, H. Miyoshi, T. Tsutsumi, T. Miyazawa, K. Ishibashi, T. Horie, K. Imai, T. Todoroki, S. Kimura, and K. Koike.** 2001. Oxidative stress in the absence of inflammation in a mouse model for hepatitis C virus-associated hepatocarcinogenesis. Cancer Res. **61**:4365–4370.
41. **Nakajima, K., Y. Yamanaka, K. Nakae, H. Kojima, M. Ichiba, N. Kiuchi, T. Kitaoka, T. Fukada, M. Hibi, and T. Hirano.** 1996. A central role for STAT3 in IL-6-induced regulation of growth and differentiation in M1 leukemia cells. EMBO J. **15**:3651–3658.
42. **Naldini, L., U. Blömer, P. Gallay, D. Ory, R. Mulligan, F. H. Gage, I. M. Verma, and D. Trono.** 1996. In vivo gene delivery and stable transduction of nondividing cells by a lentiviral vector. Science **272**:263–267.
43. **Okuda, M., K. Li, M. R. Beard, L. A. Showalter, F. Scholle, S. M. Lemon, and S. A. Weinman.** 2002. Mitochondrial injury, oxidative stress, and antioxidant gene expression are induced by hepatitis C virus core protein. Gastroenterology **122**:366–375.
44. **Pion, M., R. Stalder, R. Correa, B. Mangeat, G. J. Towers, and V. Piguet.** 2007. Identification of an arsenic-sensitive block to primate lentiviral infection of human dendritic cells. J. Virol. **81**:12086–12090.
45. **Porter, A. C., G. R. Fanger, and R. R. Vaillancourt.** 1999. Signal transduction pathways regulated by arsenate and arsenite. Oncogene **18**:7794–7802.
46. **Roederer, M., F. J. T. Staal, P. A. Raju, S. W. Ela, L. A. Herzenberg, and L. A. Herzenberg.** 1990. Cytokine-stimulated human immunodeficiency virus replication is inhibited by *N*-acetyl-L-cysteine. Proc. Natl. Acad. Sci. USA **87**:4884–4888.
47. **Saenz, D. T., W. Teo, J. C. Olsen, and E. M. Poeschla.** 2005. Restriction of feline immunodeficiency virus by Ref1, Lv1, and primate TRIM5α proteins. J. Virol. **79**:15175–15188.
48. **Sakurai, T., T. Kaise, and C. Matsubara.** 1998. Inorganic and methylated arsenic compounds induce cell death in murine macrophages via different mechanisms. Chem. Res. Toxicol. **11**:273–283.
49. **Sarcar, B., A. K. Ghosh, R. Steele, R. Ray, and R. B. Ray.** 2004. Hepatitis C virus NS5A mediated STAT3 activation requires co-operation of Jak1 kinase. Virology **322**:51–60.
50. **Sayah, D. M., and J. Luban.** 2004. Selection for loss of Ref1 activity in human cells releases human immunodeficiency virus type 1 from cyclophilin A dependence during infection. J. Virol. **78**:12066–12070.
51. **Shen, Z. X., G. Q. Chen, J. H. Ni, X. S. Li, S. M. Xiong, Q. Y. Qiu, J. Zhu, W. Tang, G. L. Sun, K. Q. Yang, Y. Chen, L. Zhou, Z. W. Fang, Y. T. Wang, J. Ma, P. Zhang, T. D. Zhang, S. J. Chen, Z. Chen, and Z. Y. Wang.** 1997. Use of arsenic trioxide ($As_2O_3$) in the treatment of acute promyelocytic leukemia (APL). II. Clinical efficacy and pharmacokinetics in relapsed patients. Blood **89**:3354–3360.
52. **Soignet, S. L., P. Maslak, Z. G. Wang, S. Jhanwar, E. Calleja, L. J. Dardashti, D. Corso, A. DeBlasio, J. Gabrilove, D. A. Scheinberg, P. P. Pandolfi, and R. P. Warrell, Jr.** 1998. Complete remission after treatment of acute promyelocytic leukemia with arsenic trioxide. N. Engl. J. Med. **339**:1341–1348.
53. **Staal, F. J. T., M. Roederer, L. A. Herzenberg, and L. A. Herzenberg.** 1990. Intracellular thiols regulate activation of nuclear factor κB and transcription of human immunodeficiency virus. Proc. Natl. Acad. Sci. USA **87**:9943–9947.
54. **Staal, F. J. T., S. W. Ela, M. Roederer, M. T. Anderson, L. A. Herzenberg, and L. A. Herzenberg.** 1992. Glutathione deficiency and human immunodeficiency virus infection. Lancet **339**:909–912.
55. **Tardif, K. D., K. Mori, and A. Siddiqui.** 2002. Hepatitis C virus subgenomic replicons induce endoplasmic reticulum stress activating an interacellular signaling pathway. J. Virol. **76**:7453–7459.
56. **Tavalai, N., P. Papior, S. Rechter, M. Leis, and T. Stamminger.** 2006. Evidence for a role of the cellular ND10 protein PML in mediating intrinsic immunity against human cytomegalovirus infections. J. Virol. **80**:8006–8018.
57. **Turelli, P., V. Doucas, E. Craig, B. Mangeat, N. Klages, R. Evans, G. Kalpana, and D. Trono.** 2001. Cytoplasmic recruitment of INI1 and PML on incoming HIV preintegration complexes: interference with early steps of viral replication. Mol. Cell **7**:1245–1254.
58. **Wakita, T., T. Pietschmann, T. Kato, T. Date, M. Miyamoto, Z. Zhao, K. Murthy, A. Habermann, H. G. Kräusslich, M. Mizokami, R. Bartenschlager, and T. J. Liang.** 2005. Production of infectious hepatitis C virus in tissue culture from a cloned viral genome. Nat. Med. **11**:791–796.
59. **Waris, G., J. Turson, T. Hassanein, and A. Siddiqui.** 2005. Hepatitis C virus (HCV) constitutively activates STAT-3 via oxidative stress: role of STAT3 in HCV replication. J. Virol. **79**:1569–1580.
60. **Waris, G., A. Livolsi, V. Imbert, J. F. Peyron, and A. Siddiqui.** 2003. Hepatitis C virus NS5A and subgenomic replicon activate NF-κB via tyrosine phosphorylation of IkBa and its degradation by calpain protease. J. Biol. Chem. **278**:40778–40787.
61. **Wen, F., M. Y. Abdalla, C. Aloman, J. Xiang, I. M. Ahmad, J. Walewski, M. L. McCormick, K. E. Brown, A. D. Branch, D. R. Spitz, B. E. Britigan, and W. N. Schmidt.** 2004. Increased prooxidant production and enhanced susceptibility to glutathione depletion in HepG2 cells co-expressing HCV core protein and CYP2E1. J. Med. Virol. **72**:230–240.
62. **Wetzler, M., M. T. Brady, E. Tracy, Z. R. Li, K. A. Donohue, K. L. O'Loughlin, Y. Cheng, A. Mortazavi, A. A. McDonald, P. Kunapuli, P. K. Wallace, M. R. Baer, J. K. Cowell, and H. Baumann.** 2006. Arsenic trioxide affects signal transducer and activator of transcription proteins through alteration of protein tyrosine kinase phosphorylation. Clin. Cancer Res. **12**: 6817–6825.

63. **Yang, S., C. Kuo, J. E. Bisi, and M. K. Kim.** 2002. PML-dependent apoptosis after DNA damage is regulated by the checkpoint kinase hCds1/Chk2. Nat. Cell Biol. **4**:865–870.
64. **Yang, S., J. H. Jeong, A. L. Brown, C. H. Lee, P. P. Pandolfi, J. H. Chung, and M. K. Kim.** 2006. Promyelocytic leukemia activates Chk2 by mediating Chk2 autophosphorylation. J. Biol. Chem. **281**:26645–26654.
65. **Yano, M., M. Ikeda, K. Abe, H. Dansako, S. Ohkoshi, Y. Aoyagi, and N. Kato.** 2007. Comprehensive analysis of the effects of ordinary nutrients on hepatitis C virus RNA replication in cell culture. Antimicrob. Agents Chemother. **51**:2016–2027.
66. **Yoda, A., K. Toyoshima, Y. Watanabe, N. Onishi, Y. Hazaka, Y. Tsukuda, J. Tsukada, T. Kondo, Y. Tanaka, and Y. Minami.** 2008. Arsenic trioxide augments Chk2/p53-mediated apoptosis by inhibiting oncogenic Wip1 phosphatase. J. Biol. Chem. **283**:18969–18979.
67. **Yoshida, T., T. Hanada, T. Tokuhisa, K. Kosai, M. Sata, M. Kohara, and A. Yoshimura.** 2002. Activation of STAT3 by the hepatitis C virus core protein leads to cellular transformation. J. Exp. Med. **196**:641–653.
68. **Zhang, P., S. Y. Wang, and X. H. Hu.** 1996. Arsenic trioxide treated 72 cases of acute promyelocytic leukemia. Chin. J. Hematol. **17**:58–62.
69. **Zhu, H., X. Shang, N. Terada, and C. Liu.** 2004. STAT3 induces anti-hepatitis C viral activity in liver cells. Biochem. Biophys. Res. Commun. **324**:518–528.
70. **Zhu, J., M. H. M. Koken, F. Quignon, M. K. Chelbi-Alix, L. Degos, Z. Y. Wang, Z. Chen, and H. de Thé.** 1997. Arsenic-induced PML targeting onto nuclear bodies: implications for the treatment of acute promyelocytic leukemia. Proc. Natl. Acad. Sci. USA **94**:3978–3983.
71. **Zufferey, R., D. Nagy, R. J. Mandel, L. Naldini, and D. Trono.** 1997. Multiply attenuated lentiviral vector achieves efficient gene delivery in vivo. Nat. Biotechnol. **15**:871–875.

Arch Virol (2009) 154:77–85
DOI 10.1007/s00705-008-0282-8

ORIGINAL ARTICLE

# Genetic variability and diversity of intracellular genome-length hepatitis C virus RNA in long-term cell culture

**Nobuyuki Kato · K. Abe · K. Mori · Y. Ariumi · H. Dansako · M. Ikeda**

Received: 28 September 2008 / Accepted: 11 November 2008 / Published online: 10 December 2008


**Abstract** Hepatitis C virus (HCV) is known to circulate persistently in vivo as a complex population of different but closely related viral variants. To understand the quasispecies nature of HCV, we performed genetic analysis of intracellular HCV RNAs obtained in long-term cell culture of genome-length HCV-RNA-replicating cells. The results revealed that genetic mutations in HCV RNAs accumulated in a time-dependent manner, and that the mutation rates of HCV RNAs were 3.5–4.8 × $10^{-3}$ base substitutions/site/year. The mutation rates of nonstructural regions that are essential for RNA replication were lower than those of structural regions. The genetic diversity of HCVs was also enlarged in a time-dependent manner. Furthermore, we found that the GC content of HCV RNA was increased in a time-dependent manner. These results suggest that an HCV-RNA-replicating cell culture system would be useful for analysis of the evolutionary dynamics and variations of HCV.

## Introduction

Hepatitis C virus (HCV) infection frequently causes chronic hepatitis, which progresses to liver cirrhosis and hepatocellular carcinoma. Such persistent infection has now become a serious health problem, with more than 170 million people worldwide currently infected with HCV [23]. HCV is an enveloped, positive single-stranded RNA (9.6 kb) virus belonging to the family *Flaviviridae*, and the HCV genome encodes a large polyprotein precursor of approximately 3,000 amino acid (aa) residues [9]. This polyprotein is cleaved by a combination of the host and viral proteases into at least 10 proteins in the following order: core, envelope 1 (E1), E2, p7, non-structural protein 2 (NS2), NS3, NS4A, NS4B, NS5A, and NS5B [5, 6, 8].

The most characteristic feature of the HCV genome is its remarkable diversity and variation. To date, more than six genotypes and multiple subtypes, which show more than 20% difference at the nucleotide level compared with any of the other subtypes, have been identified worldwide [4, 19]. An approximately 5–8% difference at the nucleotide level is observed within a single genotype [8]. Furthermore, an approximately 1% difference at the nucleotide level is also observed among HCV genomes in an individual [20]. Regarding variations of the HCV genome, three reports using specimens from chimpanzees [16, 18] and a human patient [17] have estimated that the mutation rate of the HCV genome was 1.4–1.9 × $10^{-3}$ base substitutions/site/year. Since the selective pressure of the immune system functions in vivo [10, 24], an experimental system of HCV replication is needed to define the actual mutation frequency of HCV RNA.

We considered that the cell-culture-based HCV replicon system developed in 1999 [15] would be useful as an experimental system for analysis of the genetic variations and diversity of HCV, since it has been shown that HCV subgenomic RNA (so-called replicon RNA) containing the NS3–NS5B regions could autonomously and efficiently replicate in a human hepatoma cell line, HuH-7, using this

**Electronic supplementary material** The online version of this article (doi:10.1007/s00705-008-0282-8) contains supplementary material, which is available to authorized users.

N. Kato (✉) · K. Abe · K. Mori · Y. Ariumi · H. Dansako · M. Ikeda
Department of Tumor Virology,
Okayama University of Graduate School of Medicine,
Dentistry, and Pharmaceutical Sciences, 2-5-1 Shikata-cho,
Okayama 700-8558, Japan
e-mail: nkato@md.okayama-u.ac.jp

HCV replicon system [3]. The replicon RNA is a selectable, bicistronic HCV RNA with the first cistron, the neomycin phosphotransferase ($Neo^R$) gene, being translated under control of the HCV internal ribosome entry site (IRES) and the second cistron, the NS3–NS5B regions, being translated under control of the encephalomyocarditis virus (EMCV) IRES. Therefore, we previously performed genetic analyses of HCV variation and diversity using HCV replicon systems [11, 13] developed using two HCV strains, 1B-1 and HCV-O [12]. In that study, HCV-replicon-harboring cells were cultured for 18 months (1B-1 strain) or 12 months (HCV-O strain), and, using these cell cultured specimens, the mutation rates of both HCV replicons were estimated to be approximately $3.0 \times 10^{-3}$ base substitutions/site/year. The genetic diversity of both replicons was also enlarged during long-term cell cultures [12]. However, it is unclear that the obtained results reflect the variations and diversity of the whole HCV genome, since the HCV replicon lacks the core–NS2 regions (half of the HCV genome). Furthermore, information regarding the genetic variation and diversity of the core–NS2 regions is needed in order to understand the dynamics of the whole HCV genome. To clarify this point, recently established genome-length HCV RNA (HCV-O strain)-replicating cell lines, HuH-7-derived O, OA, OB, OD, and OE [1, 7], were used for this study. There is no evidence that infectious HCV particles are released into the supernatants of genome-length HCV-RNA-replicating cells (O–OE). Since genome-length HCV-RNAs possessing cell-line-specific adaptive mutations that enhance the efficiency of RNA replication efficiently replicated in these five kinds of cells, we cultured these cells for 2 years and comprehensively analyzed the variations and diversity of the whole intracellular HCV genome. Here, we report the evolutionary HCV dynamics occurring in long-term replication of genome-length HCV RNAs.

## Materials and methods

### Cell cultures

The O, OA, OB, OD, and OE cells supporting genome-length HCV RNAs were cultured in Dulbecco's modified Eagle's medium supplemented with fetal bovine serum (10%) and G418 (0.3 mg/ml). These cells were passaged every 7 days for 2 years.

### Northern blot analysis

Total RNAs from the cultured cells were prepared using an RNeasy extraction kit (Qiagen, Hilden, Germany). Total RNA (3 μg) was used to detect the genome-length HCV RNA and β-actin mRNA (for check the amount of RNA). Northern blotting and hybridization were performed using a positive-stranded HCV-genome-specific RNA probe (NS5B region) and a β-actin-specific probe, as described previously [12].

### Quantification of HCV RNA

The reverse transcription (RT)-quantitative PCR (RT-qPCR) analysis for HCV RNA was performed using LightCycler PCR as described previously [8]. Experiments were done in triplicate.

### Western blot analysis

The preparation of cell lysates, SDS-PAGE, and immunoblotting analysis with a PVDF membrane were performed as described previously [6]. The antibodies used to examine the expression levels of HCV proteins were those against core [CP9, CP11, and CP14 monoclonal antibodies (Institute of Immunology, Tokyo); a polyclonal antibody (a generous gift from Dr. M. Kohara, Tokyo Metropolitan Institute of Medical Science, Japan)], E1 and NS5B (generous gifts from Dr. M. Kohara, Tokyo Metropolitan Institute of Medical Science, Japan). The epitopes of CP9, CP11, and CP14 were located within aa positions 39–74, 21–40, and 5–40 of the core protein, respectively. Anti-β-actin antibody (AC-15; Sigma, St. Louis, MO) was also used to detect β-actin as an internal control. Immunocomplexes on the membranes were detected by enhanced chemiluminescence assay (Renaissance; Perkin-Elmer Life Sciences, Boston, MA).

### RT-PCR and sequencing

To amplify genome-length HCV RNA, RT-PCR was performed separately in two fragments as described previously [7]. Briefly, one fragment covered from 5′-UTR to NS3, with a final product of approximately 5.1 kb, and the other fragment covered from NS2 to NS5B, with a final product of approximately 6.1 kb. These fragments overlapped at the NS2 and NS3 regions and were used for sequence analysis of the HCV open reading frame (ORF) after cloning into pBR322MC [11]. SuperScript II (Invitrogen, Carlsbad, CA) and KOD-plus DNA polymerase (Toyobo, Osaka, Japan) were used for RT and PCR, respectively. Plasmid inserts were sequenced in both the sense and antisense directions using Big Dye terminator cycle sequencing on an ABI PRISM 310 genetic analyzer (Applied Biosystems, Foster City, CA). The nucleotide sequences of each of the three independent clones obtained were determined.

### Molecular evolutionary analysis

Nucleotide and deduced amino acid sequences of the clones obtained by RT-PCRs were analyzed by neighbor-joining analysis using the program GENETYX-MAC (Software Development, Tokyo, Japan).

## Results

### Efficient replication of genome-length HCV RNA is maintained in long-term cell culture

To prepare the specimens for the genetic analysis of HCV, genome-length HCV-RNA-replicating O, OA, OB, OD, and OE cells were cultured for 2 years. The cell-line-specific and conserved adaptive mutations, K1609E, E1202G, P1115L, Q1112R, and P1115L, in the NS3 region were detected in the O, OA, OB, OD, and OE cells, respectively, when these cell lines were established [1, 7]. Using the specimens obtained at 0, 1, and 2 years in culture of O, OA, OB, OD, and OE cells, the levels of genome-length HCV RNAs were examined by Northern blot analysis (Fig. 1a) and RT-qPCR analysis (Fig. 1b). As shown in Fig. 1a, genome-length HCV RNAs approximately 11 kb long were detected in all specimens except that from HuH-7 parental cells, although the strength of the detected bands was weak in some cases. However, RT-qPCR analysis revealed that at least approximately $2 \times 10^7$ copies/μg RNA were present in the cultured cells (Fig. 1b). The results of RT-qPCR were well correlated with those of Northern blot analysis. The levels of HCV proteins (core, E1, and NS5B) were also examined by Western blot analysis. The E1 and NS5B proteins were also detected in all specimens except that from HuH-7 cells, although the levels of E1 protein were rather different among the specimens (Fig. 1c). In contrast, core protein was not detected in OB1, OB2, and OE2 cells, when the mixture of three kinds of monoclonal antibodies (CP9, CP11, and CP14) was used for the analysis. Even when polyclonal anti-core antibody was used, core protein was still not detected in OB2 cells. In addition, the strength of bands detected in the Western blot analysis was decreased in a time-dependent manner. These results suggest that sequence variations within the epitopes of the anti-core or E1 antibody, but not the anti-NS5B antibody, have occurred during the long-term cell culture.

### Genetic variations of genome-length HCV RNAs during long-term cell culture

The determined nucleotide sequences of genome-length HCV RNAs were compared with those of the original ON/C-5B RNA (Gene Bank accession no. AB191333) [7] used for the establishment of the O, OA, OB, OD, and OE cell lines. The results revealed that the numbers of base substitutions in genome-length HCV RNAs increased in a time-dependent manner (Fig. 2). These substitutions were considered to be mutations that occurred during the intracellular replication of genome-length HCV RNA. Based on the results after 2 years in culture, the apparent mutation rates of genome-length HCV RNAs in O, OA, OB, OD, and OE cells were calculated to be $3.5 \pm 0.4$, $4.5 \pm 1.4$, $4.8 \pm 0.6$, $4.3 \pm 0.5$, $4.2 \pm 0.4 \times 10^{-3}$ base substitutions/site/year, respectively. These values suggest that the genetic evolution of HCV in these different cell lines occurs at similar rates during long-term RNA replication. The deduced aa substitution rates in HCV ORFs among these cell lines are well correlated with the mutation rates of HCV RNAs (Fig. 2). We further examined whether or not the mutation rates are similar throughout the HCV genome. For this analysis, genome-length HCV RNA was divided into three parts: the 5′-terminus to the EMCV IRES region (1,938 nts), the core to the NS2 region (3,078 nts), and the NS3 to the NS5B region (5,955 nts). The results revealed that the mutation rates in the NS3–NS5B regions were lower than those of the other regions, although the 5′-terminus to the EMCV IRES region in the OA and OE cell lines showed mutation rates similar to that for the NS3–NS5B regions (Fig. 3). These results suggest that the NS3–NS5B regions, which are essential for RNA replication, are evolutionally limited. The conserved aa substitutions (mutated in all three clones sequenced) are summarized in Table 1 (core–p7 regions) and Table 2 (NS2–NS5B regions). Eight aa substitutions (K12N, Q1112R, P1115L, K1609E, A1738T, K2280E, D2292E, and D2415G) were commonly detected in at least two different cell lines. Approximately 57% of aa substitutions detected in this study were found in the Hepatitis Virus Database (http://s2as02.genes.nig.ac.jp; Nagoya City University, Japan).

### Classification of mutations occurring in genome-length HCV RNAs during the long-term cell culture

We examined the numbers of synonymous and non-synonymous mutations with transition or transversion in three divided regions ($Neo^R$, core–NS2, and NS3–NS5B regions). The results revealed that the frequencies of aa substitutions in the NS3–NS5B regions were lower than those in the core–NS2 regions, and that the rate of transition mutations in genome-length HCV RNA was greater than the rate of transversion mutations (Supplementary Table S1), as previously reported for the replicon system [12].

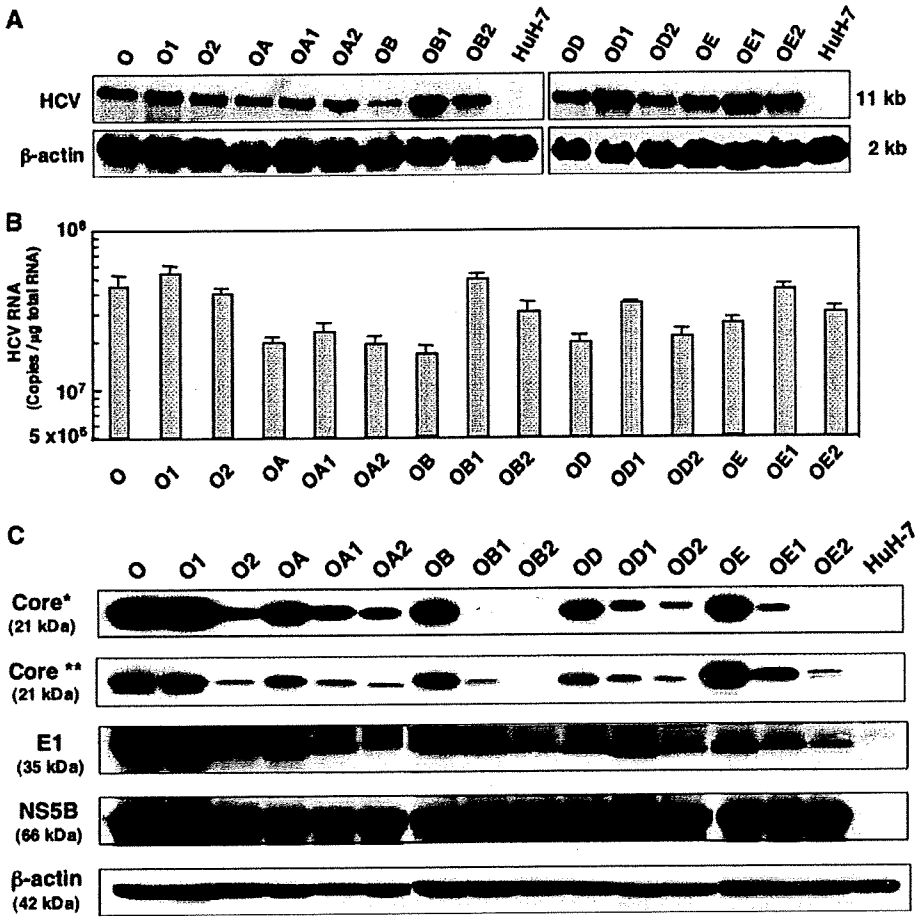


**Fig. 1** Characterization of cells containing replicating genome-length HCV RNA in long-term cell culture. **a** Northern blot analysis. Total RNAs from O, OA, OB, OD, and OE cells after 1 year (O1, OA1, OB1, OD1, and OE1) and 2 years (O2, OA2, OB2, OD2, and OE2) in culture, as well as total RNAs from the parental O, OA, OB, OD, and OE cells were used for the analysis. HuH-7 cells were used as a negative control. In vitro-synthesized ON/C-5B RNA [1] was used as a size marker (11 kb). **b** Quantitative analysis of intracellular genome-length HCV RNA. The total RNAs from the cells used for Northern blot analysis were also used for comparison. The levels of intracellular genome-length HCV RNA were quantified by Light-Cycler PCR. **c** Western blot analysis. The cellular lysates from the cells used for Northern blot analysis were also used for comparison. Core, E1, and NS5B were detected by Western blot analysis. β-actin was used as a control for the amount of protein loaded per lane. A *single star* indicates that the mixture of three kinds (CP9, CP11, and CP14) of anti-core monoclonal antibodies was used for detection. A *double star* indicates that the anti-core polyclonal antibody was used for detection

Also regarding the mutation patterns, U → C and A → G mutations were the most and second-most frequent mutations, and these mutations were two to three times more frequent than C → U and G → A mutations (Supplementary Table S2) as previously reported in the replicon analysis [12]. The rarest mutation was C → G in 1- and 2-year cultures (Supplementary Table S2). As a result, we observed that the GC content of HCV RNA gradually increased in a time-dependent manner. The increase in GC content was observed in all genome-length HCV RNAs obtained from cultured cell lines (Fig. 4).

## Genetic diversity of genome-length HCV RNA arising during long-term cell culture

Based on the sequence data of all clones obtained after 2-year culture, we examined the genetic diversities of genome-length HCV RNAs by the construction of phylogenetic trees. The results revealed that the genetic diversities of genome-length HCV RNAs were expanded at both the nucleotide and aa sequence levels, as previously reported in the replicon analysis [12], and that the three clones derived from each cell line were clustered and located at similar genetic distances from the origin

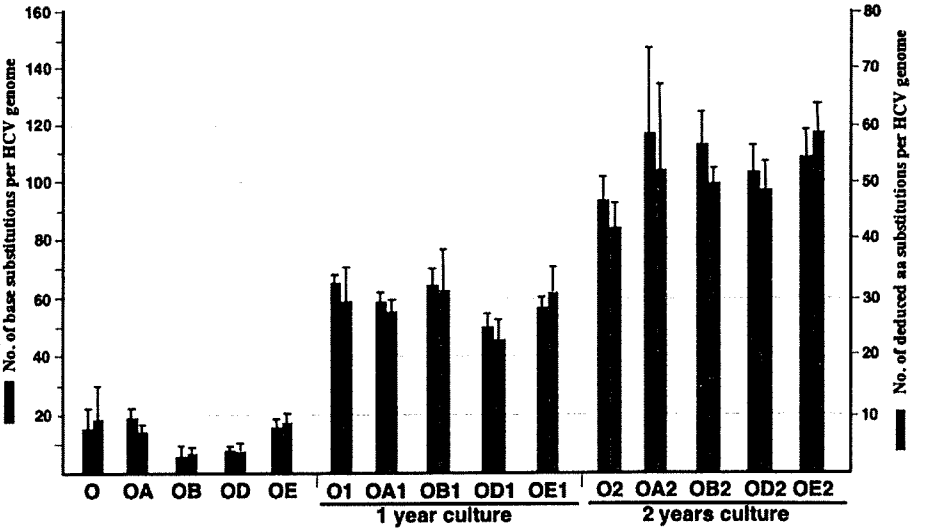


**Fig. 2** Genetic variations occurring in long-term replication of genome-length HCV RNAs. The *left vertical line* indicates the mean numbers of base substitutions detected in three clones of genome-length HCV RNA, by comparison with the original sequences (ON/C-5B) [7]. The *right vertical line* indicates the mean numbers of aa substitutions deduced from each of three clones of genome-length HCV RNA, by comparison with the original aa sequences (ON/C-5B) [7]

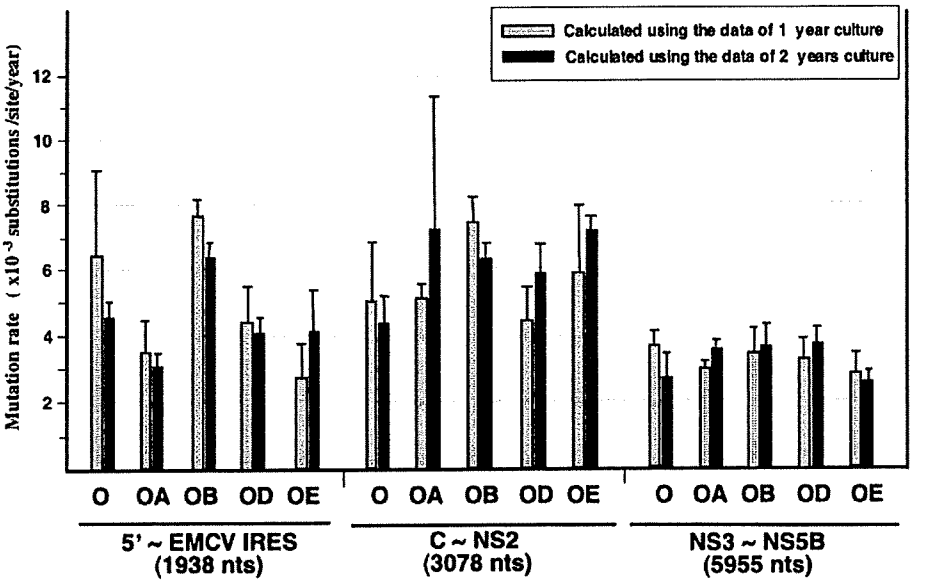


**Fig. 3** Mutation rates of genome-length HCV RNAs in long-term cell culture. The mutation rates of three regions (5′–EMCV-IRES, Core–NS2, and NS3–NS5B) of genome-length HCV RNAs (O, OA, OB, OD, and OE) were calculated using the sequence data obtained from 1- or 2-year cell culture. The *vertical line* indicates the means of the mutation rates calculated using the nucleotide sequences of three clones of genome-length HCV RNAs, by comparison with the original sequences (ON/C-5B) [7]

(ON/C-5B) at both the nucleotide and aa sequence level (Supplementary Fig. S1). These results indicate that the quasispecies nature of genome-length HCV RNA has been steadily acquired over long-term intracellular RNA replication.

## Discussion

In the present study, we analyzed the genetic evolution and dynamics of HCV in long-term culture of five kinds of genome-length HCV-RNA-replicating cells, and demonstrated that the genetic mutations of HCV accumulated in a time-dependent manner, and the genetic diversity of HCV also increased with time. These results will be useful for understanding the quasispecies nature of HCV in patients with chronic hepatitis C.

Previously, we reported that the genetic mutation rate of HCV replicons (subgenomic RNA) was approximately $3.0 \times 10^{-3}$ base substitutions/site/year in both the 5′ terminus–EMCV IRES region and the NS3–NS5B regions [12]. The NS3–NS5B regions in this study showed mutation rates ($2.8–3.8 \times 10^{-3}$ base substitutions/site/year) similar to those of the replicons in the previous study; however, the mutation rates of the 5′ terminus to the EMCV IRES region in O and OB cells were over $6.0 \times 10^{-3}$ base substitutions/site/year, suggesting that genetic mutations in this region occur independently

**Table 1** Conserved aa substitutions occurring during long-term replication of genome-length HCV RNAs (I)

| Region | aa Substitution | Observed cells | Region | aa Substitution | Observed cells | Region | aa Substitution | Observed cells |
|---|---|---|---|---|---|---|---|---|
| Core | S2G | OB2 | Core | N163S | O2 | E2 | A457T[a] | OB1, OB2 |
| | K6N | OB2 | | N163T | OE1, OE2 | | D463H[a] | OE, OE1, OE2 |
| | K10R[a] | OB2 | | L169S | OD1, OD2 | | W469R | OE2 |
| | K10E | OA2 | | F174S | O2 | | Y485H | OA1, OA2 |
| | K12N[a] | OA1, OA2 | | F177S | OB1, OB2 | | Y485C | OD2 |
| | | OE2 | | | | | G504S | OE2 |
| | N16D | OE1, OE2 | E1 | N205T | O2 | | Y507H | OA2 |
| | F24V | OB2 | | D218G[a] | OB2 | | L537P | OB2 |
| | V34A | OD2 | | M219V[a] | OB1, OB2 | | M555V[a] | OB1 |
| | R40G | O2 | | I220V[a] | OE1, OE2 | | T595A[a] | OA2 |
| | L44M[a] | OE2 | | C226R[a] | OE2 | | K595A[a] | OA2 |
| | T49A[a] | OE2 | | L242I[a] | OE2 | | K596N | OD1, OD2 |
| | K67M[a] | O2 | | T257A[a] | OA1, OA2 | | L603S | OE2 |
| | P71S[a] | O2 | | I258K | OE, OE1, OE2 | | C607S | OA1, OA2 |
| | A75P | OE2 | | L264S[a] | O2 | | G649E | OE2 |
| | A77T | OB2 | | C272R[a] | OE2 | | D658G[a] | OD1, OD2 |
| | A77P | OD2 | | S273P[a] | O2 | | T670A[a] | OB2 |
| | E89V[a] | O2 | | R296H[a] | OD1 | | I674T[a] | O2 |
| | R101C | OE2 | | Q302R[a] | OA1, OA2 | | L689S | OA1, OA2 |
| | T110M[a] | OE1, OE2 | | V313A[a] | OB2 | | N695S | OE2 |
| | L119S | OB2 | | Y361C[a] | OA2 | | V713L | OA1, OA2 |
| | K121R | OD1, OD2 | | Y361H | OE, OE1, OE2 | | Y718H | OB1, OB2 |
| | I123T[a] | O2 | | V381D | OA2 | | Y718C | OD1 |
| | F130L[a] | OA1, OA2 | | | | | L722P | O2 |
| | L133F | OB2 | E2 | G389R | OE2 | | | |
| | L139P | OE1, OE2 | | F437S | OD1, OD2 | p7 | F771S | OE2 |
| | | | | | | | L796P | O2 |

[a] aa Substitutions found in the Hepatitis Virus Databasse (http://s2as02.genes.nig.ac.jp; Nagoya City University, Japan)

among these cell lines. It was also noticed that the mutation rates ($4.3–7.4 \times 10^{-3}$ base substitutions/site/year) in the core–NS2 regions became higher than those in the NS3–NS5B regions due to frequent mutations in the core, E1, and E2 regions (Table 1). It was particularly difficult to detect the core protein by Western blot analysis due to the genetic changes within epitopes for anti-core antibodies (Fig. 1c). These results suggest that the structural region including the core, E1, and E2 regions is not required for persistent intracellular RNA replication, although approximately 42% of the aa substitutions detected in this study were observed in HCV-infected persons (Table 1). However, since we have recently found that DDX3 DEAD-box RNA helicase, which binds to the N-terminal domain (aa 1–59) of the core protein, is required for efficient replication of genome-length HCV RNA in O cells [2], none of the mutations detected in the core region should impair the interaction with DDX3. Furthermore, 6 and 9N-glycosylation sites in the E1 and E2 proteins, respectively, were completely conserved even after 2 years in culture, indicating that the E1 and E2 proteins may also affect the efficiency of RNA replication. Therefore, we speculate that the aa substitutions detected in the structural region do not reflect all of the random mutations occurring in long-term RNA replication. In contrast to the numerous aa substitutions in the structural region, the hypervariable region (HVR) 1 located in the N-terminal region of the E2 protein showed only one aa substitution (G389R in OE2 cells). This finding supports our previous proposition that an immunosurveillance system is involved in the genetic mutation in HVR1 [10]. In addition, no aa substitutions were detected in HVR2 (aa 474–480) of the E2 protein.

We showed that the mutation rates of HCV RNAs were $3.5–4.8 \times 10^{-3}$ base substitutions/site/year. However, our observed mutation rates of the HCV RNAs were 1.8–3.4 times higher than those previously obtained in chimpanzees [16, 18] and a human patient [17] with chronic hepatitis C. Since the selective pressures of the humoral immune responses [10] targeting the envelope proteins and cellular immune responses [24] targeting all HCV proteins

**Table 2** Conserved aa substitutions occurring during long-term replication of genome-length HCV RNAs (II)

| Region | aa Substitution | Observed cells | Region | aa Substitution | Observed cells | Region | aa Substitution | Observed cells |
|---|---|---|---|---|---|---|---|---|
| NS2 | M814T[a] | OE1, OE2 | NS4B | L1724I[a] | OB2 | NS5A | D2377G[a] | OA2 |
| | I885V[a] | O2 | | A1738T[a] | OA2 | | V2385H[a] | OD2 |
| | F886L | OB2 | | | OD1, OD2 | | S2387P | OD1, OD2 |
| | E887G[a] | O2 | | | OE2 | | L2391P | OA2 |
| | T889A | OB2 | | I1797V[a] | OB2 | | W2405R[a] | OE2 |
| | I891V[a] | O2 | | P1822S | OE2 | | E2414G[a] | OB2 |
| | L902F[a] | OB2 | | V1880A | OA1, OA2 | | D2415G[a] | OA, OA1, OA2 |
| | M939V[a] | OE, OE1, OE2 | | | | | | OD1, OD2 |
| | | | NS5A | S1975T[a] | OE2 | | C2418R[a] | OA2 |
| NS3 | Q1112R[a, b] | O1, O2 | | H2218R[a] | OE2 | | | |
| | | OB2 | | H2219R[a] | OB2 | NS5B | N2529S[a] | OB2 |
| | | OD, OD1, OD2 | | S2221F[a] | OA2 | | N2536S[a] | OB2 |
| | P1115L[a, b] | OB, OB1, OB2 | | N2248D[a] | OB2 | | V2757A[a] | OB2 |
| | | OE, OE2 | | K2280E[a] | OB2 | | K2860R[a] | OB2 |
| | N1148S[a] | OE2 | | | OD1, OD2 | | R2963Q[a] | OB2 |
| | E1202G[a, b] | OA, OA1, OA2 | | A2284T | OB2 | | W2990R | O2 |
| | T1531A[a] | OA2 | | D2292E[a] | OB2 | | V3002A | O2 |
| | D1581E[a] | OA2 | | | OE2 | | | |
| | K1609E[a, b] | O, O1, O2 | | V2340M[a] | OA2 | | | |
| | | OE2 | | S2342P[a] | OD2 | | | |
| | I1612T[a] | OD1, OD2 | | G2371A[a] | OE2 | | | |
| | I1641M[a] | OD1, OD2 | | G2376S[a] | OD1, OD2 | | | |

[a] aa Substitutions found in the Hepatitis Virus Database (http://s2as02.genes.nig.ac.jp; Nagoya City University, Japan)

[b] Adaptive mutations detected in O, OA, OB, OD, and OE cells when these cell lines were established [1, 7]

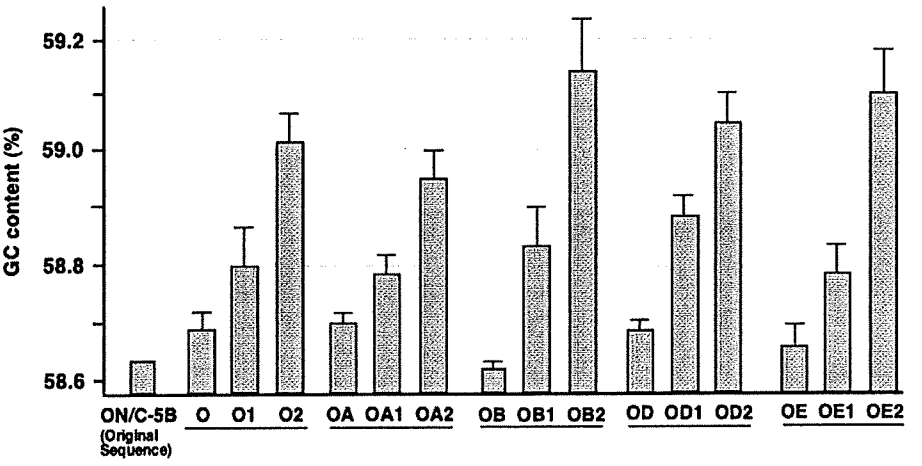


**Fig. 4** Increased GC content of genome-length HCV RNAs in long-term cell culture. The GC content of genome-length HCV RNAs (O–O2, OA–OA2, OB–OB2, OD–OD2, and OE–OE2) was calculated. The values indicate the means of three clones of each genome-length HCV RNA

function in vivo, the mutation rates obtained in this study using the cell culture system without the immunological pressure would be reasonable values as a potential mutation rate of HCV in RNA replication.

It is noteworthy that none of the aa substitutions were detected in the N-terminal half (242 aa of aa 1,976–2,217) of the NS5A protein after 2 years in cell cultures. This finding suggests that this region is the most critical for maintenance of RNA replication. It is interesting that this region corresponds to domain I (aa 1,973–2,185), which has been shown to complex with a zinc ion [21] and exists as a dimer [22]. Since the mutation of four cysteine residues essential for binding to zinc ions results in the complete inhibition of RNA replication [21], the complete